Optimized Mold Temperature Control

Table of contents

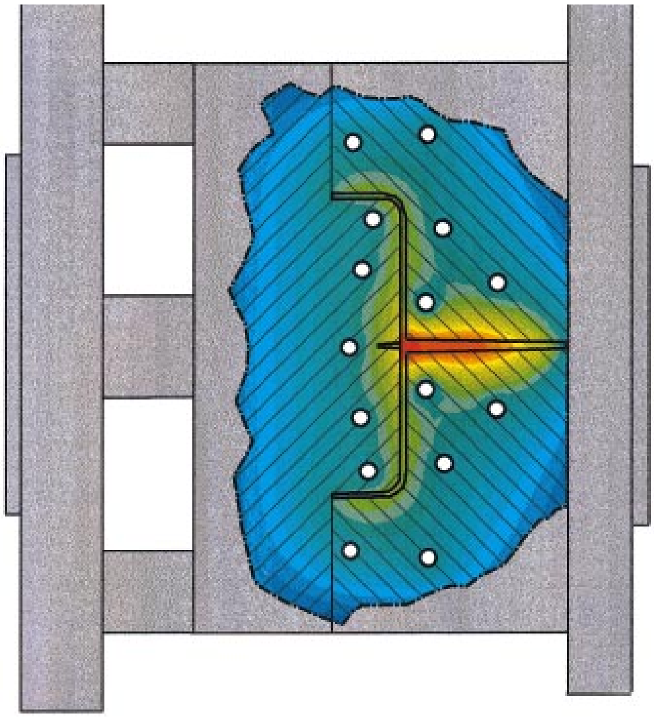

www.plastics.covestro.com
Edition 2016-03

1 Introduction

Injection molds are some of the most expensive items of industrial equipment in use, being subject both to fluctuating loads and to stringent accuracy requirements. An injection mold must be of a sound design if it is to fulfil the economic requirements placed upon it.

The cost-efficiency of an injection mold is dictated primarily by the efficiency and speed of the heat exchange between the mold and the molding compound injected into it.

The quality of the molded part depends to a decisive extent on a consistent local temperature progression from one cycle to the next. The decisive factor determining the cost-efficiency of production is whether the mold is a good or a poor conductor of heat.

When it comes to processing, optimized mold temperature control is the most important parameter for reducing unit costs. The savings potential of an improved mold temperature control system is 10 – 40 %.

If the quality of the molded part is to be enhanced and production time reduced, it is necessary to understand the laws that govern the exchange of heat in the mold and deliberately exploit these.

The correlations presented in this brochure are intended to illustrate why the thermal design of the mold has to be perceived as a key stage in the design process. Readers are also shown that if they use the design aids that are available (equations, nomograms, diagrams and computer programs), it is no longer necessary for the thermal design of the mold to be carried out on the basis of "the more heating/cooling channels, the better!".

2 Why the need for a heating/cooling system for the mold?

The raw materials manufacturers who supply the thermoplastics generally specify both an optimum processing temperature (or temperature range) and the best mold temperatures for their products.

In many cases, the recommended temperatures for the mold are not observed. Processors prefer to work at low temperatures in order to save on cycle time, turning a blind eye to the fact that this can impair the quality of the molded parts.

How are the recommended temperatures that are set out in Fig. 1 below obtained, and why is it necessary for a mold to be heated and cooled at all?

When thermoplastics are injection molded, hot molten plastic is periodically injected into a "cold" mold. Hence, it has to be assumed that if there were no heating/cooling system, the mold would heat up on account of the heat content of the molten plastic before reaching and maintaining a certain temperature level. However, it is scarcely possible to predict what this temperature level would be and how long it would take to develop.

Fig. 2 shows the mold surface temperature during start-up in qualitative terms, both with and without a mold heating/cooling system. Without a heating/cooling system, the time taken for quasi steady-state temperature conditions to be achieved is much greater. With a mold heating/cooling system, the desired, uniform temperature on the mold surface is attained relatively rapidly.

How important is it for a specific temperature level to prevail at the cavity surface? This "specific temperature level" is a parameter that can have a particularly decisive influence on molded part quality in terms of:

– surface appearance
– shrinkage
– inherent stresses
– uniform structure
– geometry and dimensional deviations

A number of examples will be given in order to underline the importance of a correctly selected cavity surface temperature.

Thermoplastic	Mold temperature in °C	Melt temperature in °C	Demolding temperature in °C
Apec® HT (PC-HT) 150	100 – 150	310 – 340	150
Bayblend® (PC+ABS)	(55)[1] 70 – 100	240 – 280	110
Desmopan® (TPU)	20 – 50	190 – 245	50 – 70
PA 66 PA 66, GF PA 6 PA 6, GF	(60)[1] 80 – 100 (60)[1] 80 – 120 (60)[1] 80 – 100 (60)[1] 80 – 120	275 – 295 280 – 300 260 – 280 270 – 290	110 140 100 130
Makrolon® (PC) Makrolon® (PC, GF)	(>65)[1] 80 – 100 (>65)[1] 80 – 130	280 – 320 310 – 330	<140 <150
ABS	(>45)[1] 60 – 80	220 – 260	80 – 100
SAN	50 – 80	230 – 260	80 – 95
PBT PBT, GF	(>60)[1] 80 – 100	250 – 270	<140 <150
ABS + PA	80 – 100	250 – 270	90 – 100

Fig. 1: Recommended mold, melt and demolding temperatures for different thermoplastics [1]

[1] Values achieved in practice with allowance for costs and quality

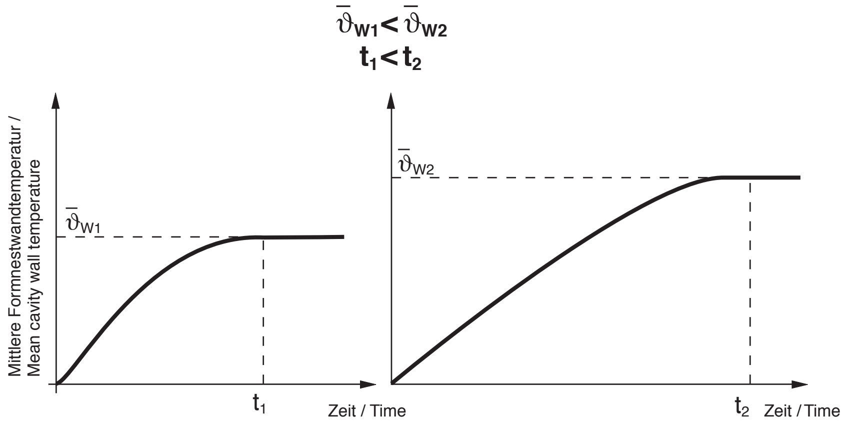

Fig. 2: Cavity wall temperature, start-up phases with (left) and without (right) mold heating

To achieve a high level of crystallinity which extends right through to the surface layers of molded parts in the case of semi-crystalline molding compounds, it is necessary to work with high cavity wall temperatures. Excessively rapid cooling (achieved through a lower mold cavity temperature) will hinder crystallization [2].

Fig. 3 shows that the degree of crystallization falls sharply if the cavity wall temperature is set at a low level. This will result in post-crystallization and post-shrinkage in the course of time.

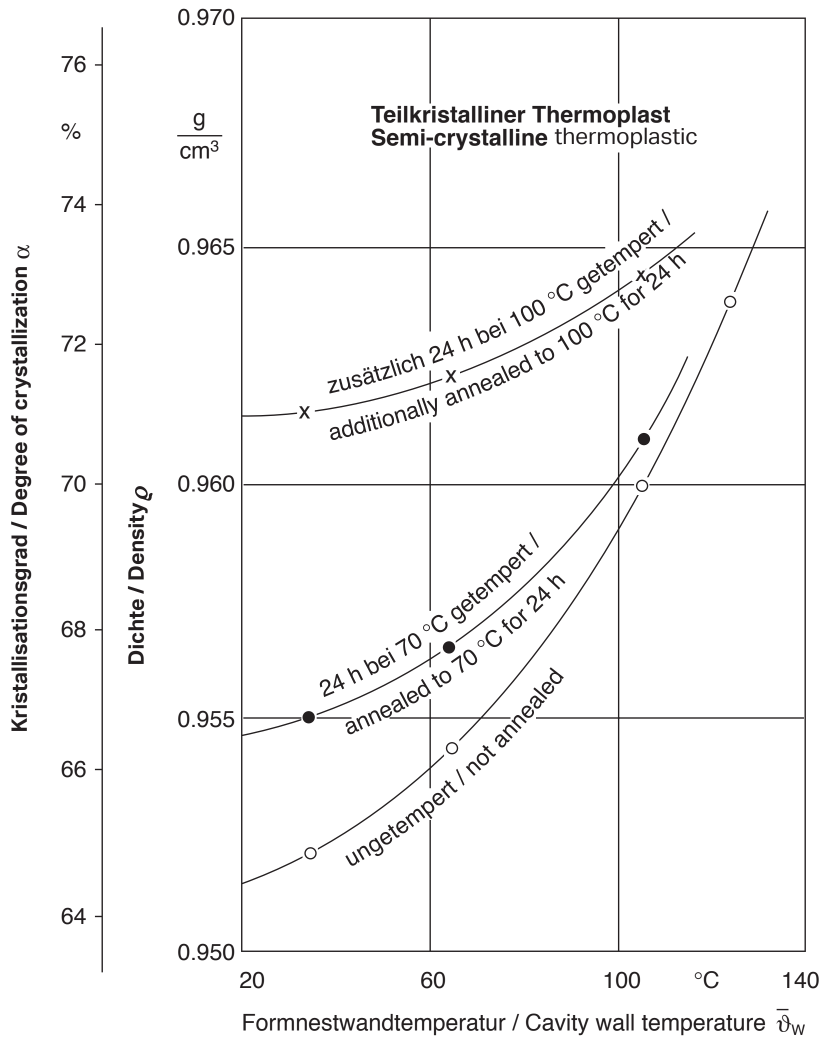

Fig. 3: Influence of cavity wall temperature and annealing on the density and degree of crystallization of injection molded parts [2]

Fig. 4 illustrates the way in which material shrinkage is influenced by the cavity wall temperature. This Figure shows the overall shrinkage (made up of the molding shrinkage and the post-shrinkage) as a function of the cavity temperature for a non-reinforced polyamide 6. It is very clear that, with a very low cavity temperature (ϑ_W = 40 °C), the molding shrinkage component undergoes a pronounced fall while the post-shrinkage undergoes a corresponding increase. The overall shrinkage potential remains unchanged. Molded parts in polyamide which are produced with too low a cavity temperature have a high post-shrinkage potential and hence a high potential for subsequent shape and dimensional deviations which are difficult to predict.

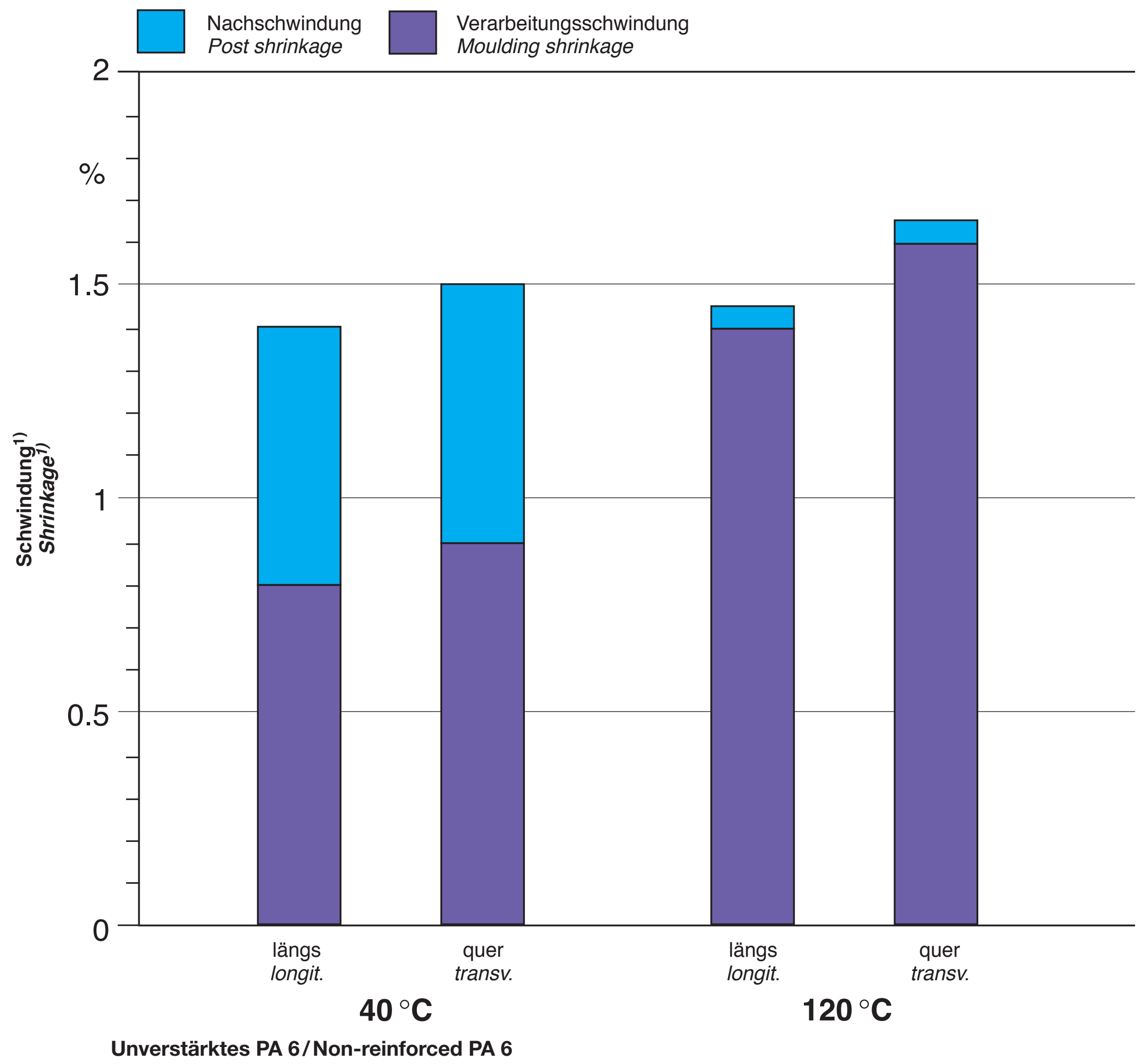

Fig. 4: Molding shrinkage and post-shrinkage as a function of cavity wall temperature for PA 6, non-reinforced

[1)] Plate 150 x 90 x 3 mm

Fig. 5 highlights the positive influence of a higher cavity wall temperature on the formation of the structure in layers close to the surface. With the high cavity wall temperature, an almost uniform structure forms right up to the edge of the molded part.

In addition to low cavity wall temperatures causing the potential suppression of crystallization in semi-crystalline materials (through high cooling rates), the stress state prevailing in the molding is also a function of the cavity wall temperature. Fig. 6 shows that the corners of a molded part, which are susceptible to stress cracking, display a lower level of stress when produced with high cavity wall temperatures.

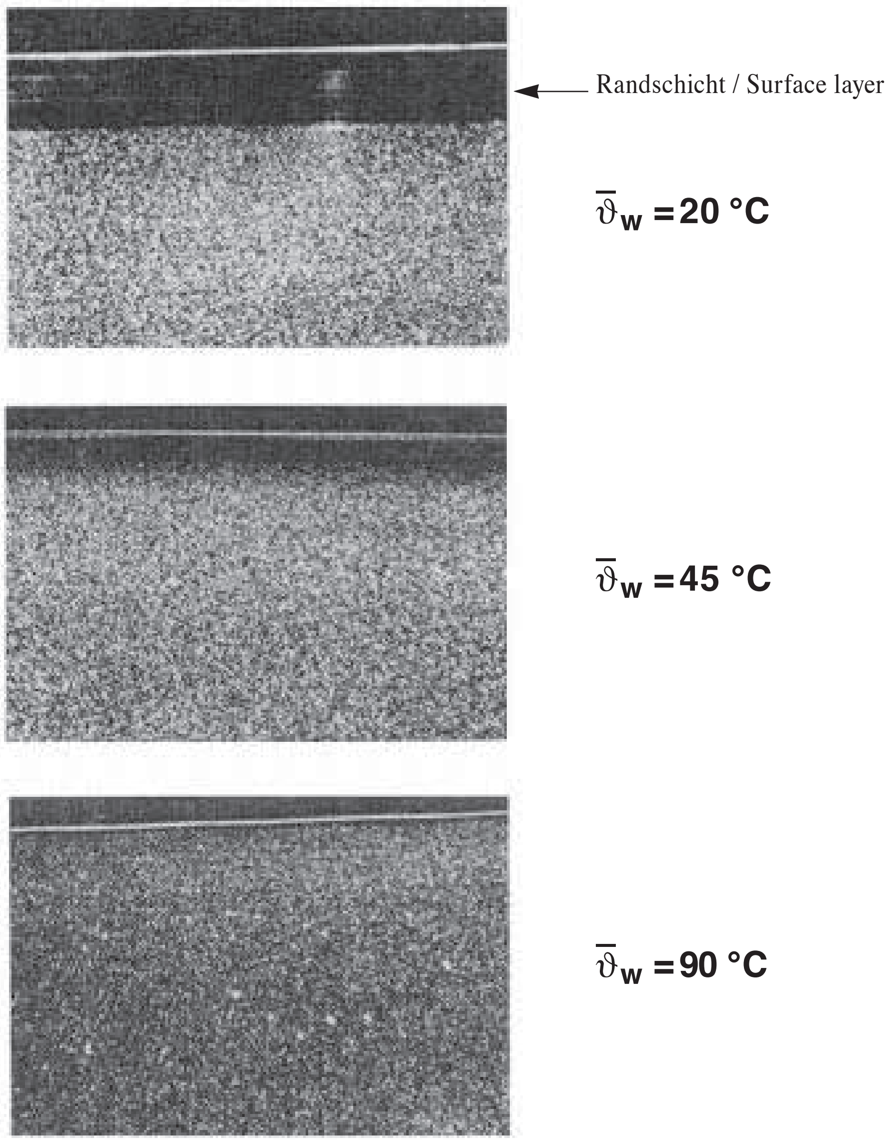

Fig. 5: Structure in the surface layers of semi-crystalline injection moldings produced with different cavity wall temperatures [2]

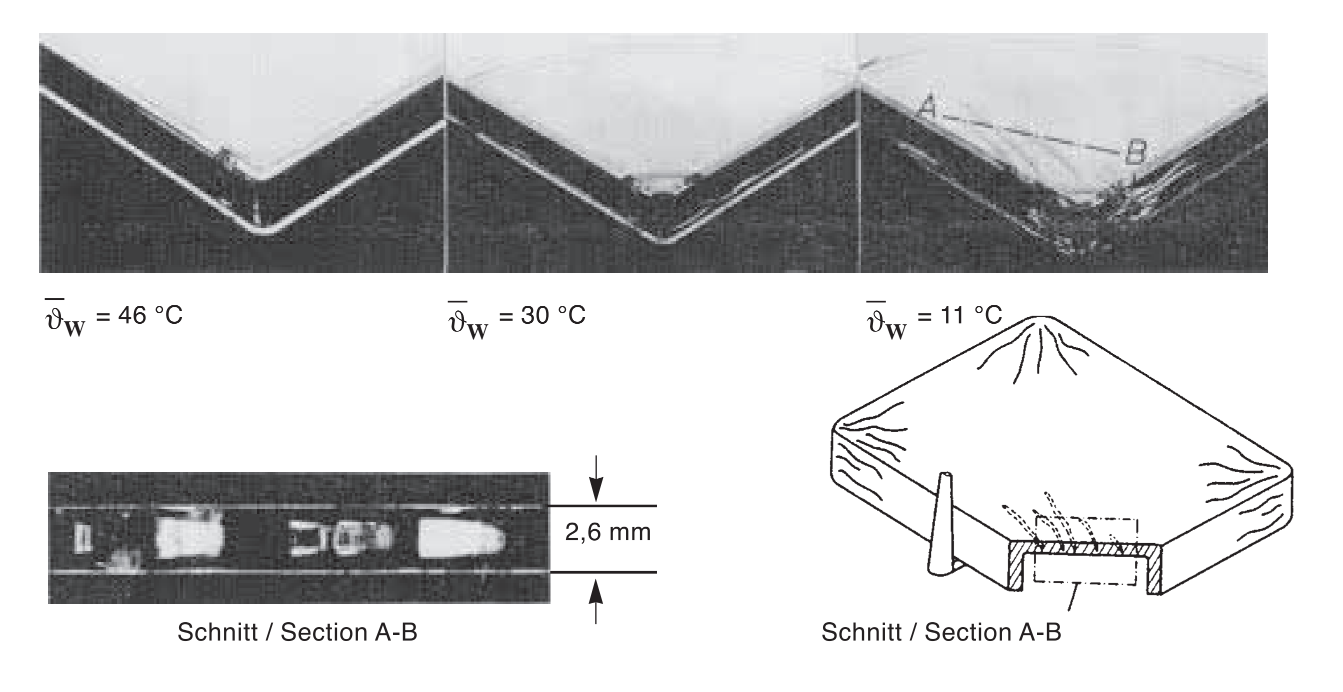

Fig. 6: Stress cracks in an amorphous molding as a function of the cavity temperature ϑ_W in the corners of the molded part following storage in n-heptane [2]

As Fig. 6 shows, higher cavity surface temperatures can reduce the amount of stress cracking. Cracks of this type can be triggered by inherent stresses (mechanical stresses that prevail in the molded part without external loading). Most of the inherent stress is accounted for by inherent cooling stress, the development of which is described in a highly comprehensible manner by Stitz's solidification model (Fig. 7, right-hand side).

The pronounced temperature profile that prevails in the solidifying melt during cooling (a) gives rise to a dissimilar thermal contraction potential in the different layers (b). The mechanical link that exists between the individual layers prevents them from sliding freely over each other and gives rise to a mean contraction (c). The impeded thermal expansion leads to the development of internal strains over the cross-section of the molding.

It is possible to specify an approximation equation for the cooling strain, according to Knappe [3], which shows a parabolic strain profile over the molding cross-section (Fig. 7, left-hand side). The tensile phase of the cooling strain is located in the core of the molding, whilst the compression phase, which maintains the equilibrium, is located in the outer layers.

Fig. 6 confirms Knappe's equation for the cooling strain in qualitative terms. According to this equation, the level of the stress is simply a function of the difference between the glass transition temperature and the applied cooling temperature, i. e. the cavity wall temperature in this case. When using this equation, it must be borne in mind that the Young's modulus and the coefficient of expansion are a function of the temperature.

$$\sigma = -\frac{2}{3}\,\alpha E\,(\vartheta_E - \vartheta_A)\left(\frac{6x^2}{s^2} - \frac{1}{2}\right)$$

σ = Spannung / Stress

α = Ausdehnungskoeffizient / Coefficient of expansion

E = E-Modul / Young's modulus

ϑ_E = Einfriertemperatur / Freezing temperature

ϑ_A = Abschrecktemperatur / Quenching temperature

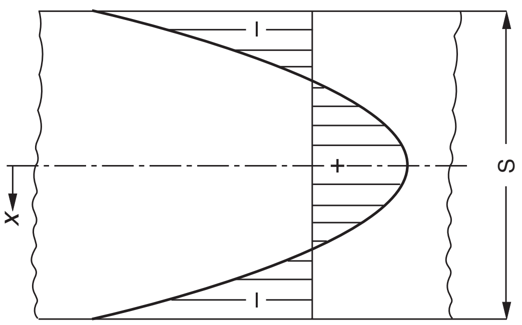

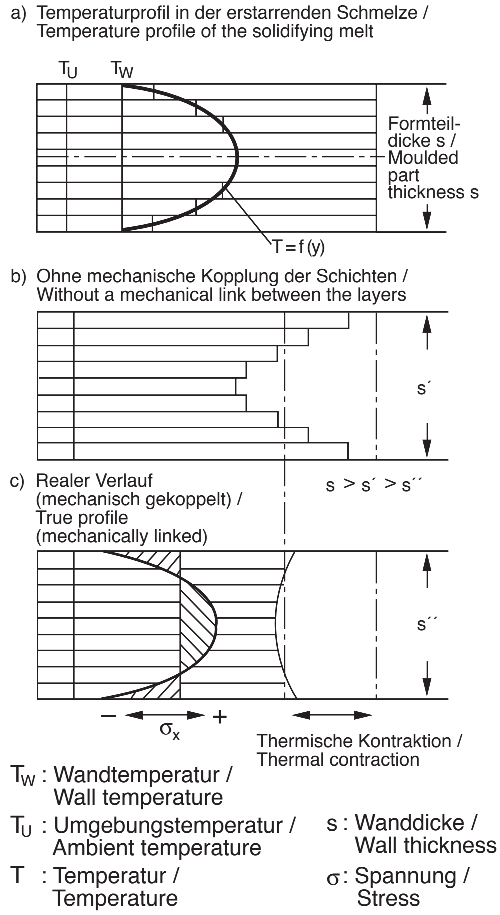

Fig. 7: Cooling stresses according to Knappe [3], thermal contraction and the development of inherent stresses according to Stitz [4]

For the sake of completeness it should be pointed out that the internal cooling stresses can also have flow-conditioned internal stresses superimposed on them which originate in stretching flow effects at the flow front, as well as internal stresses which result from an overpacked cavity with subsequent demolding under residual pressure (stresses due to expansion).

The accuracy with which the surface of the cavity is reproduced is determined not only by the melt viscosity and the processing conditions (e.g. injection velocity) but, in particular, by the cavity wall temperature. Fig. 8 shows the degree of gloss of an ABS mirror housing as a function of the cavity wall temperature. With a higher cavity temperature, the fine-grained structure is reproduced more efficiently, the reflected light is diffused more uniformly and the surface gives more of a matt impression.

In the case of glass-fibre reinforced thermoplastics, it is essential to ensure that the melt covers the glass fiber at the surface, since these will otherwise be visible and make the molding look as if it has a "gray veil" placed over it. This is best achieved by employing not only a high injection rate but also high cavity wall temperatures (Fig. 9).

Fig. 8: Gloss difference, conditioned by the cavity wall temperature; mirror housing in ABS [5]

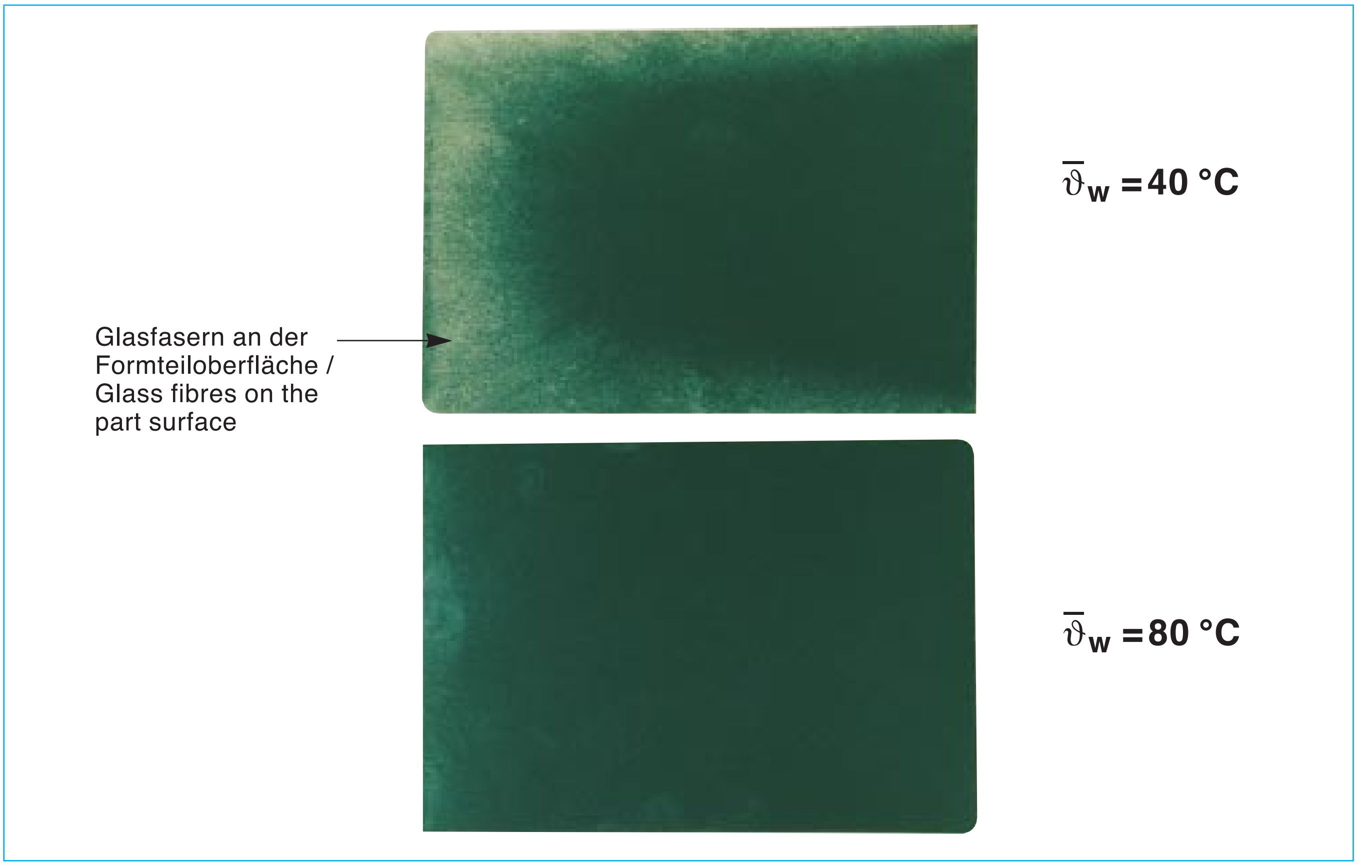

Fig. 9: Surface appearance of injection moldings in PA 6, GF30 as a function of cavity surface temperature

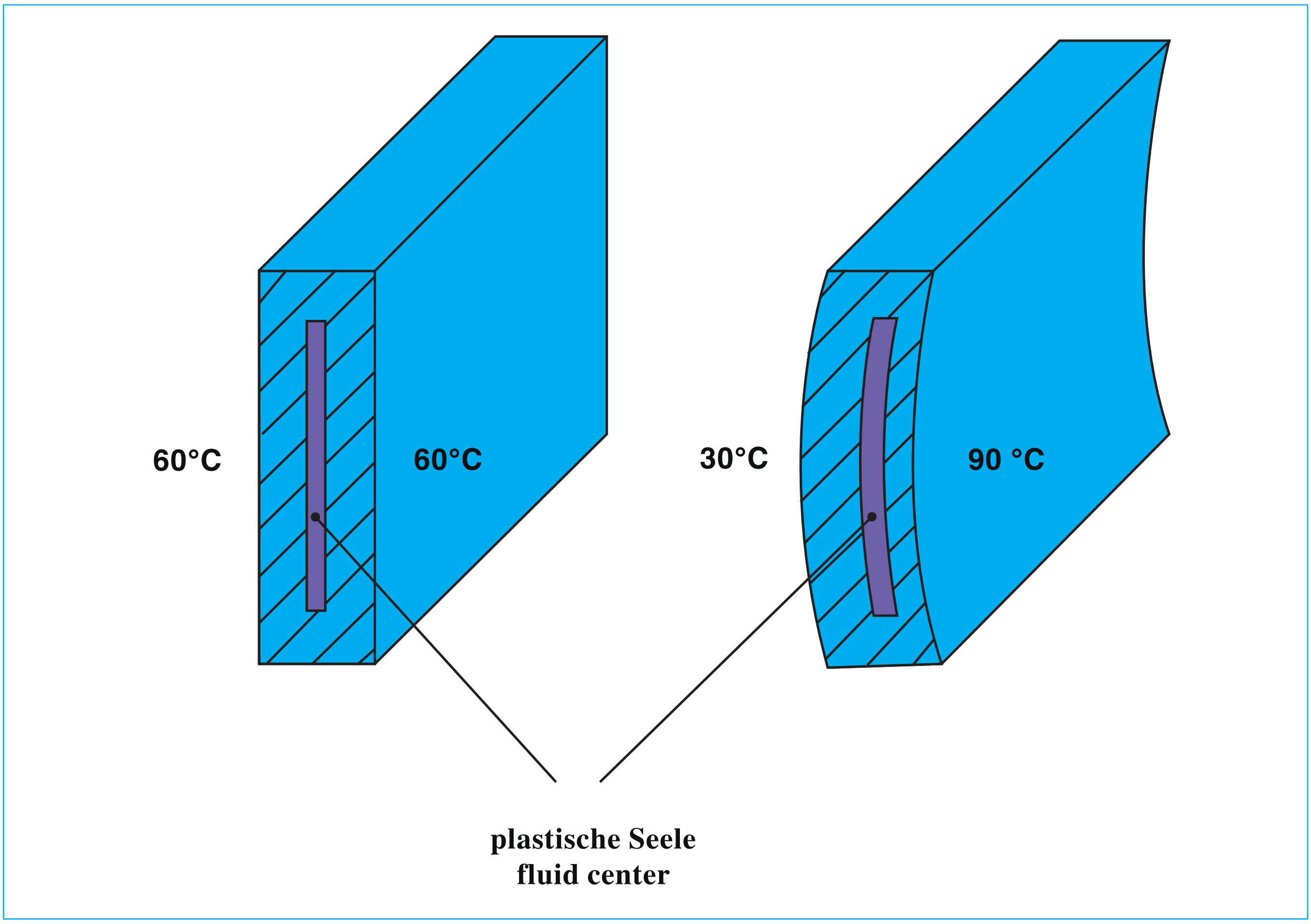

Fig. 10: Influence of the cavity surface temperature on the warpage of non-reinforced thermoplastics

Warpage in plastics moldings is caused by shrinkage differentials in the molded part. Apart from these shrinkage differentials, together with wall thickness differences and orientation (of glass fibers), molded part warpage can be triggered by the cavity surface temperature giving rise to differential shrinkage. This applies particularly in the case of flat parts.

Figure 10 shows how a flat part becomes deformed through different cavity temperatures prevailing on the top and bottom sides. Shrinkage is suppressed on the mold side with the low temperature, and the side with the high temperature undergoes more pronounced shrinkage. A type of bi-metal effect occurs.

3 Aims of thermal mold design

On the basis of the examples that have been given, the following aims can be specified for the mold heating/cooling system:

1. The target mean cavity wall temperature (either an empirical value or the value specified by the raw materials manufacturer) is to be maintained as precisely as possible.
2. The temperature prevailing at the mold surface should be as uniform as possible at the different points, otherwise inconsistent molded part properties and warpage may result.
3. The cooling time and hence the cycle time must be as short as possible in order to ensure a high cost-efficiency for a given molded part quality.

4 Temperature profile at the cavity surface, mean cavity wall temperature

In the preceding section, mention was made of a mean cavity wall temperature, despite the fact that the mold wall temperature at any specific point in the mold will be subject to fluctuations over time (Fig. 11).

The periodic fluctuations in cavity wall temperature have physical origins (mold material, molding compound, melt temperature), and the cooling system is not able to influence the amplitude of these fluctuations.

Directly prior to injection, the mold wall temperature is ϑ_{Wmin}. When the hot plastic melt touches the colder mold wall, a contact temperature of ϑ_{Wmax} momentarily prevails. This will then fall on account of the cooling that takes place during the cycle. Fig. 12 shows a schematic diagram of the temperature equalization process that takes place between the polymer and the mold.

The temperatures measured at different times (t_1, t_2, t_3, t_4) at the measuring point in Fig. 12 can be plotted as a function of time, as is shown in Fig. 11.

The mold wall temperature undergoes a steady fall from the maximum temperature (ϑ_{Wmax} in Fig. 11) in the course of the cycle, on account of the cooling. Once the molded part has been demolded (ϑ_{WE} in Fig. 11), the fall in temperature is accelerated. At the start of the new cycle, ϑ_{Wmin} is attained again for as long as quasi steady-state operation prevails.

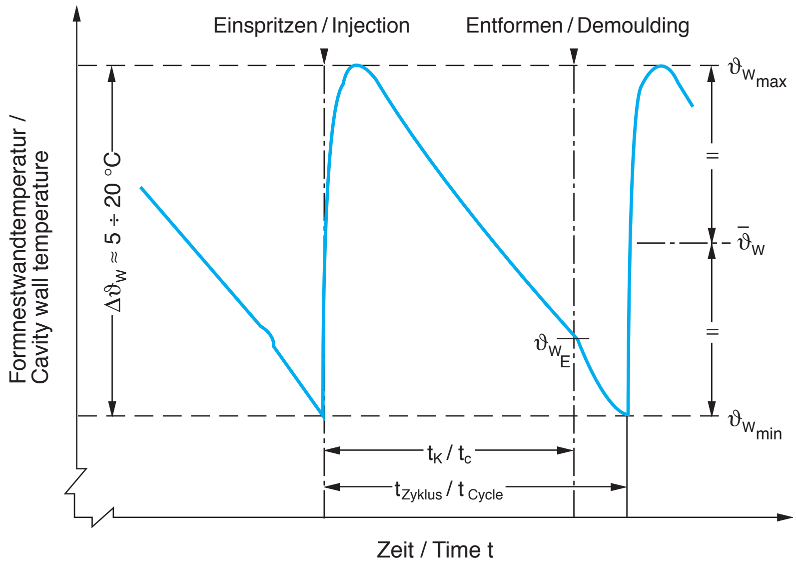

Fig. 11: Temperatures on the cavity wall of an injection mold during uninterrupted production [7]

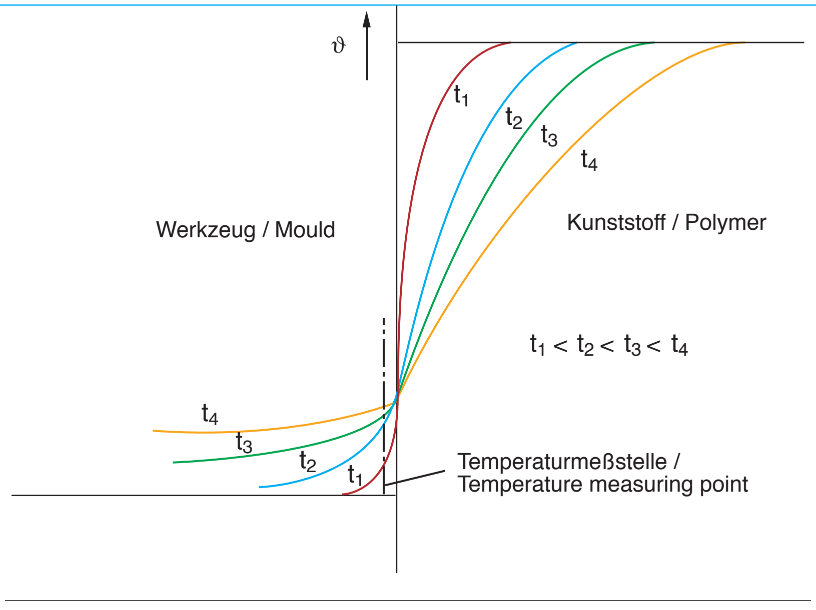

Fig. 12: Temperature equalization when two bodies at different temperatures come into contact with each other (schematic diagram) [7]

The contact temperature ϑ_{Wmax} is a function of the heat permeability b of the mold and the molding compound and can be estimated with the following equation [7]:

$$\vartheta_{Wmax} = \frac{b_W \cdot \vartheta_{Wmin} + b_M \cdot \vartheta_M}{b_W + b_M} \qquad b = \sqrt{\rho \cdot \lambda \cdot c}$$

ϑ_{Wmin} = cavity wall temperature immediately prior to injection
ϑ_M = melt temperature
b = heat permeability
b_W = heat permeability of the mold steel
b_M = heat permeability of the molding compound
ρ = density
λ = thermal conductivity
c = specific heat capacity

The heat permeability of a number of materials is set out in the Table below.

Material	Heat permeability b $Ws^{1/2}\ m^{-2}\ deg^{-1}$
Beryllium copper (BeCu 25)	$17.2 \cdot 10^3$
Unalloyed steel (C 45 W 3)	$13.8 \cdot 10^3$
Chromium steel (X 40 Cr 13)	$11.7 \cdot 10^3$
Polyethylene (PE-HD)	$0.99 \cdot 10^3$
Polystyrene (PS)	$0.57 \cdot 10^3$

Table 1: Heat permeability of a number of materials and injection molding compounds [7]

From the values set out above, it is clear that metals have a far greater heat permeability than thermoplastics. For this reason, the contact temperature ϑ_{Wmax} between the melt and the cavity wall is in the vicinity of the cavity wall temperature prior to injection, ϑ_{Wmin}. With highly alloyed steels having poor heat conduction, the contact temperature will rise to a higher level than for molds which are good conductors (beryllium-copper inserts). The outer layer of the molded part is chilled to a lesser extent, and favorable relaxation conditions prevail right through to the surface areas. It is the peak temperature ϑ_{Wmax} that is of decisive importance for the quality of the molded part. The temperature increase can be stepped up through the application of a thin heat insulation layer, thereby enhancing the reproduction of the surface at the same time.

The mean cavity surface temperature ϑ_W can be used for establishing the cooling time and also for determining the necessary cooling capacity with a sufficient degree of accuracy.

$$\overline{\vartheta}_W = \frac{\vartheta_{Wmax} + \vartheta_{Wmin}}{2}$$

For practical reasons, the minimum temperature ϑ_{Wmin} is sometimes specified as the decisive temperature in the literature, since this is the easiest temperature to measure in the injection molding shop.

This is untenable on physical grounds, however. This temperature does not prevail while the molding is in the mold but only a considerable time afterwards [2].

The amplitude of the temperature fluctuation $\Delta\vartheta_W$ falls with an increasing distance from the cavity surface. This is particularly important when it comes to the correct position of the temperature sensor in relation to the cavity surface for an externally controlled cavity wall temperature (Fig. 13).

One of the target variables in the thermal design of the mold is the mean cavity wall temperature $\overline{\vartheta}_W$ shown in Fig. 11. If this temperature is attained in (almost) all the areas of the mold, then this will ensure that identical cooling conditions prevail in respect of the heating/cooling system.

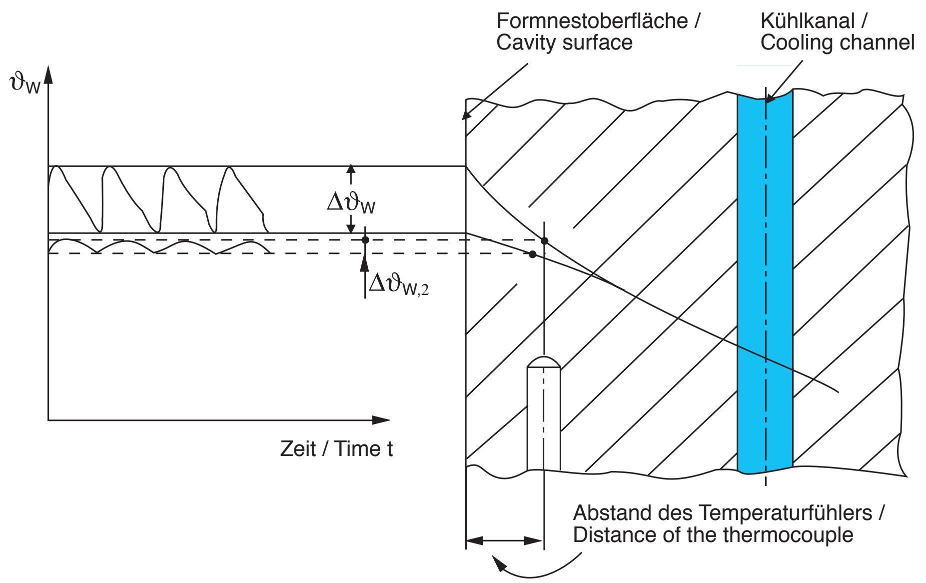

Fig. 13: Reduction in temperature amplitude in the mold [8]

5 Prerequisites for optimum temperature control of the mold

The temperature control unit, the heating/cooling channel system in the mold and the heat carrier (cooling medium) together make up the temperature control system. Specific conditions are imposed on each of the three components in order to ensure that the aims set out above can be achieved:

a) The position and number of heating/cooling channels should be selected in such a way that uniform heating/cooling is guaranteed in all areas of the molding, and a sufficiently large heating/cooling channel surface is available. Particular attention should be given to heating/cooling at the corners of the molding (to prevent corner warpage).

Dissimilar cooling rates from one point to the next lead to dissimilar solidification times and hence to dissimilar shrinkage and internal stresses. The dissimilar surface areas at corners cause considerable differences to develop:

– high cooling rates in the convex areas
– low cooling rate in the concave areas

From the diagram at the bottom of Fig. 14 it is clear that two cooling channels can be assigned to the shaded square on the outside of the corner. Three squares can be allocated to a single channel on the concave side. As a result, the molten core shifts towards the concave side. During solidification, material deficits occur, since the shrinkage is not compensated by any additional material being forced in. The result is tensile stresses which at times can lead to corner warpage subsequent to demolding. Over and above this, holes, sink marks or spontaneous cracks may occur.

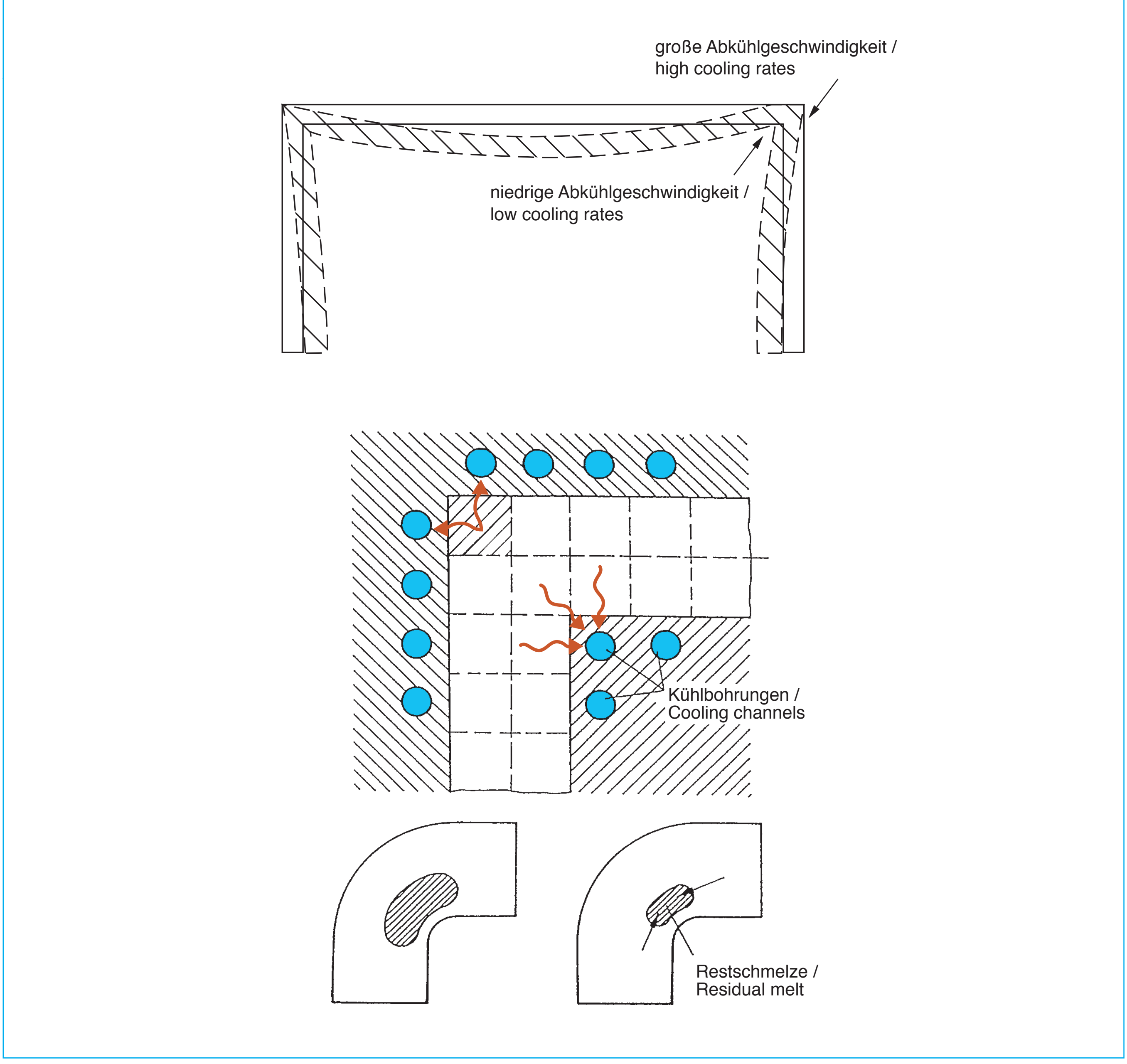

Fig. 14: Solidification of the melt in a corner of the molding [9]

The following methods can be employed to adjust the heat flows in the corners (temperature peak or residual melt thickness in the centre of the molding) and hence to reduce corner warpage:

- Cold core and hot cavity

  The low core temperature causes the core side to cool so rapidly that the residual melt is located in the centre of the corner.

  drawbacks:
  – the straight surfaces of the molded part are subject to dissmilar cooling
  – this method will not work if the core contains convex regions as well (see diagram)

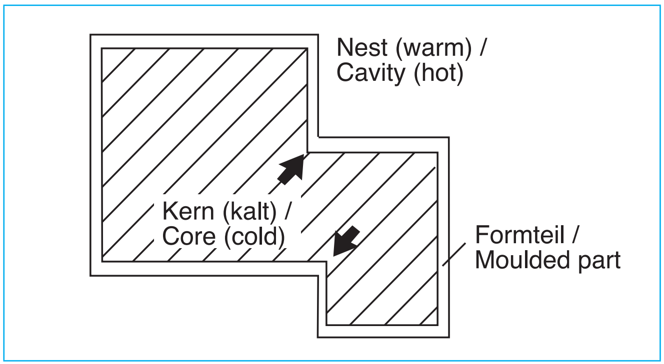

- Modification to corner geometry

  adjustment of the heat flows through:
  – a low heat content and/or
  – a bigger exchange surface

  drawbacks:
  – molding corner is weakened
  – increase in mold follow-up costs

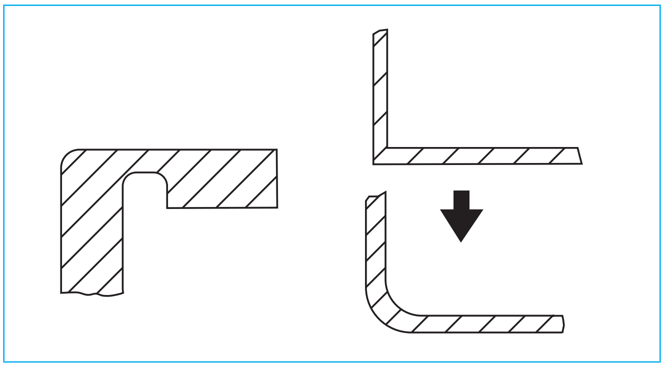

- Partial adjustment of the heat flows:

  – through the use of material with a higher thermal conductivity on the concave side of the corner (copper-beryllium inserts)

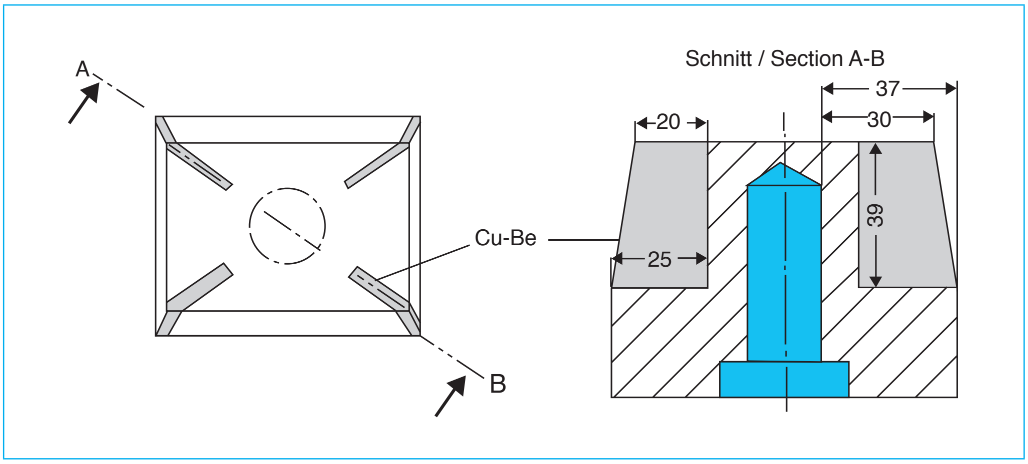

  – through the smallest possible distance between the corner and the cooling channel wall

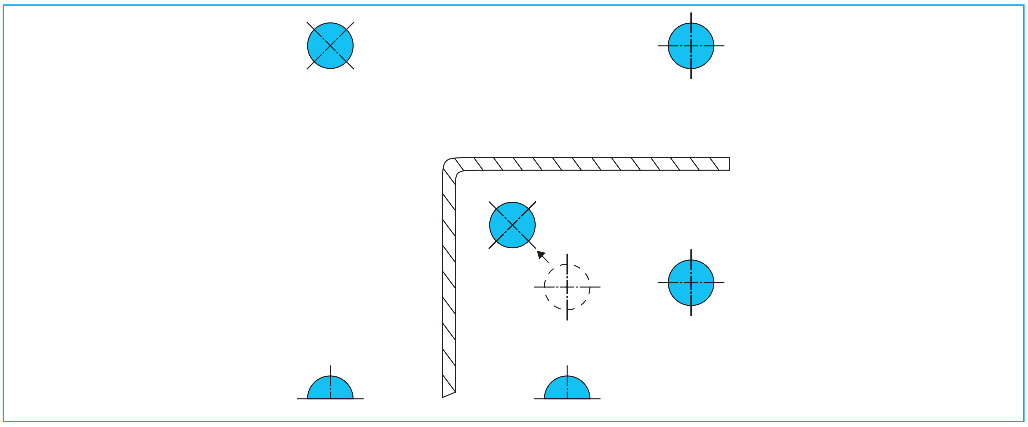

b) When determining the size of the heating/cooling channels, consideration must be paid to the pressure that is required to convey the cooling medium inside the mold. Excessively small cooling channel diameters will result in a high pressure drop. Particular importance is therefore attached to a correctly dimensioned heating, cooling and pumping capacity.

c) The temperature differential between the inflow and outflow temperature of the heat carrier (cooling medium) should be as small as possible (≤ 2 °C for precision injection moldings). In the case of high-quality molded parts, therefore, it may be necessary to employ a number of parallel circuits in order to ensure that the temperature differential does not become too pronounced.

d) The heat carrier (cooling medium) should possess good heat transfer properties; water is a suitable medium here.

If a comparison is drawn between water and heat carrier oil for the heat transfer conditions with the following settings:

– a heating/cooling-medium temperature ϑ_{TM} = 80 °C
– a channel diameter D_{KK} = 8 mm
– a heating/cooling-medium throughput $\dot{m}_{TM}$ = 5 kg/min

then the following is obtained for the coefficient of heat transfer:

water: α_{TM} = 10 900 W/m² · oil
oil: α_{TM} = 696 W/m² · K

The heat transfer conditions are thus more than ten times as good with water (for the settings employed) [7].

e) The flow conditions in the heating/cooling channel should always be turbulent (Reynolds number Re much greater than 2300). If smaller Reynolds numbers result, then it will be necessary to reduce the diameter of the cooling channel (for a specified throughput) or to employ a less viscous heating/cooling medium.

Fig. 15 below shows just how important a turbulent flow is for the heating/cooling medium. The coefficient of heat transfer α_{TM} shown in there is a decisive parameter for the efficiency of a heating/cooling system in a specified position and with a given size of heating/cooling channel. This will be all the greater the higher the Reynolds number is, i. e. the more turbulent the flow.

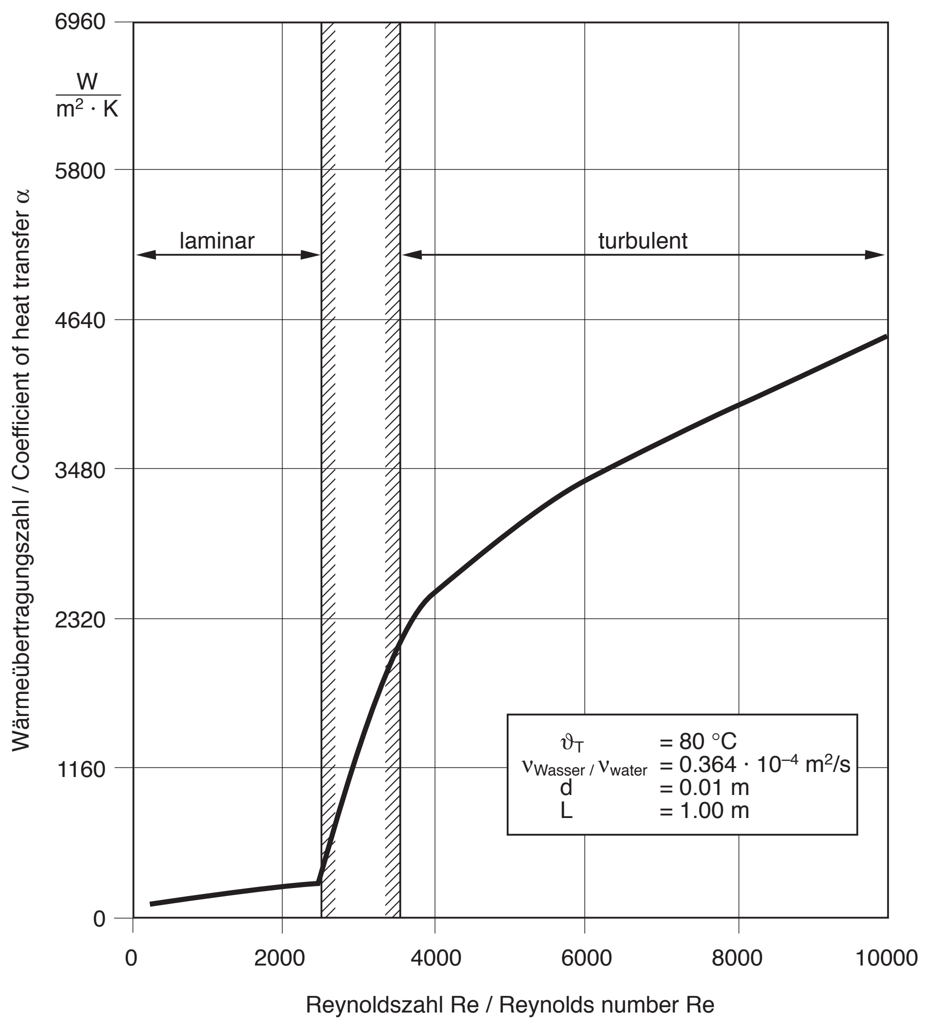

Fig. 15: Coefficient of heat transfer as a function of Reynolds number for water

f) The temperature control unit must be equipped with sufficient heating, cooling and pumping capacity and be in a position to maintain the target mean mold wall temperature within tight tolerances, irrespective of the production conditions.

g) A positive influence on cooling can be achieved through the use of an article design that is suitably tailored to plastics, coupled with an optimum design in flow engineering terms (number and position of injection points, flow paths). The requirements placed on the heating/cooling system and also its complexity can be reduced to a lower level by avoiding major differences in wall thickness and accumulations of melt (ribs, bosses).

6 Cooling time (temperature-control time)

Cooling proper commences right at the cavity filling stage. During the cooling phase, however, it is essential that the melt be prevented from freezing through the “flow heat” that is generated by internal friction (a quasi isothermal flow process). The chief quantity of heat is exchanged after the filling phase, i. e. up to the point when the mold is opened and the molding ejected from it.

The exchange of heat between the molding compound and the cooling medium takes place by heat conduction through the cavity walls. The time required for the demolding temperature to be reached (cooling time) can be estimated as a function of the molded part geometry using the simplified equations in Fig. 16.

These equations make allowance for the conduction of heat from the large surfaces to the mold wall. If the equations given in Fig. 16 are applied for short cooling times (cooling phase not very far advanced) then this can lead to considerable deviations from the actual times. For this reason, the Fourier number ought to be checked. The recommended Fourier number is > 0.05, or better still 0.1.

Dimensionless Fourier number:

$$\frac{t \cdot a}{x^2} > 0.05 \text{ better} > 0.1)$$

t = calculated cooling time from Fig. 16
a = thermal diffusivity
x = wall thickness s for plates – radius r for a cylinder with L = ∞

The effective thermal diffusivity a_{eff} used in the equations (Fig. 16) is a reference value that is taken to be constant. It leads to the same degree of cooling (over the same period of time as the actual temperature-dependent thermal diffusivity [7]. The degree of cooling is dimensionless.

$$\theta = \frac{\vartheta_M - \overline{\vartheta}_W}{\overline{\vartheta}_E - \overline{\vartheta}_W}$$

Θ = degree of cooling
$\overline{\vartheta}_E$ = mean demolding temperature
$\overline{\vartheta}_W$ = mean cavity wall temperature
ϑ_M = melt temperature after completion of mold filling

In contrast to the thermal diffusivity, the effective thermal diffusivity is then just a function of the mean mold wall temperature and the glass fiber content of the material [7].

Geometrie / Geometry	Randbedingung / Boundary condition	Gleichung / Equation	
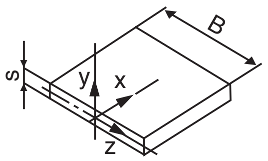	Platte / Plate $\dot{Q}_Z = 0$ $\dot{Q}_X = 0$	$t_K = \frac{s^2}{\pi^2 \cdot a_{eff}} \cdot \ln\left(\frac{8}{\pi^2} \cdot \frac{\vartheta_M - \bar{\vartheta}_W}{\bar{\vartheta}_E - \bar{\vartheta}_W}\right)$ $t_K = \frac{s^2}{\pi^2 \cdot a_{eff}} \cdot \ln\left(\frac{4}{\pi} \cdot \frac{\vartheta_M - \bar{\vartheta}_W}{\hat{\vartheta}_E - \bar{\vartheta}_W}\right)$	1 1a
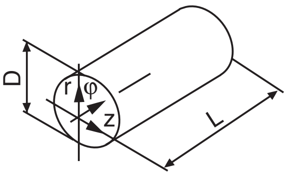	Zylinder / Cylinder $\dot{Q}_\varphi = 0$ $\dot{Q}_Z = 0$ L >> D	$t_K = \frac{D^2}{23.14 \cdot a_{eff}} \cdot \ln\left(0.692 \cdot \frac{\vartheta_M - \bar{\vartheta}_W}{\bar{\vartheta}_E - \bar{\vartheta}_W}\right)$ $t_K = \frac{D^2}{23.14 \cdot a_{eff}} \cdot \ln\left(1.602 \cdot \frac{\vartheta_M - \bar{\vartheta}_W}{\hat{\vartheta}_E - \bar{\vartheta}_W}\right)$	2 2a
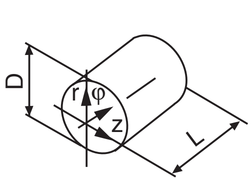	Zylinder / Cylinder $\dot{Q}_\varphi = 0$ L ~ D	$t_K = \frac{1}{\left(\frac{23.14}{D^2} + \frac{\pi^2}{L}\right) \cdot a_{eff}} \cdot \ln\left(0.561 \cdot \frac{\vartheta_M - \bar{\vartheta}_W}{\bar{\vartheta}_E - \bar{\vartheta}_W}\right)$ $t_K = \frac{1}{\left(\frac{23.14}{D^2} + \frac{\pi^2}{L}\right) \cdot a_{eff}} \cdot \ln\left(2.04 \cdot \frac{\vartheta_M - \bar{\vartheta}_W}{\hat{\vartheta}_E - \bar{\vartheta}_W}\right)$	3 3a
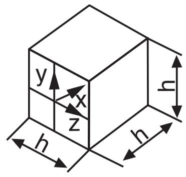	Würfel / Cube	$t_K = \frac{h^2}{3 \cdot \pi^2 \cdot a_{eff}} \cdot \ln\left(0.533 \cdot \frac{\vartheta_M - \bar{\vartheta}_W}{\bar{\vartheta}_E - \bar{\vartheta}_W}\right)$ $t_K = \frac{h^2}{3 \cdot \pi^2 \cdot a_{eff}} \cdot \ln\left(2.064 \cdot \frac{\vartheta_M - \bar{\vartheta}_W}{\hat{\vartheta}_E - \bar{\vartheta}_W}\right)$	4 4a
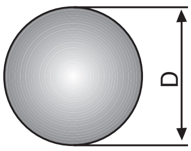	Kugel / Sphere	$t_K = \frac{D^2}{4 \cdot \pi^2 \cdot a_{eff}} \cdot \ln\left(2 \cdot \frac{\vartheta_M - \bar{\vartheta}_W}{\hat{\vartheta}_E - \bar{\vartheta}_W}\right)$	5
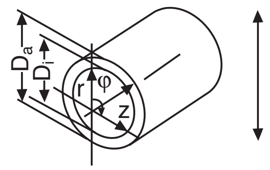	Hohlzylinder / Hollow cylinder $\dot{Q}_\varphi, \dot{Q}_z = 0$ $r < D_i/2$: $\dot{Q}_r = 0$	Gl. (1; 1a) mit $s = D_a - D_i$ / Eqn. (1; 1a) where $s = D_a - D_i$	6
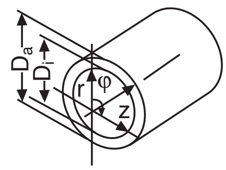	Hohlzylinder / Hollow cylinder $\dot{Q}_\varphi, \dot{Q}_z = 0$	Gl. (1; 1a) mit $s = (D_a - D_i)/2$ / Eqn. (1; 1a) where $s = (D_a - D_i)/2$	7

Fig. 16: Cooling time equations for different geometries [10]

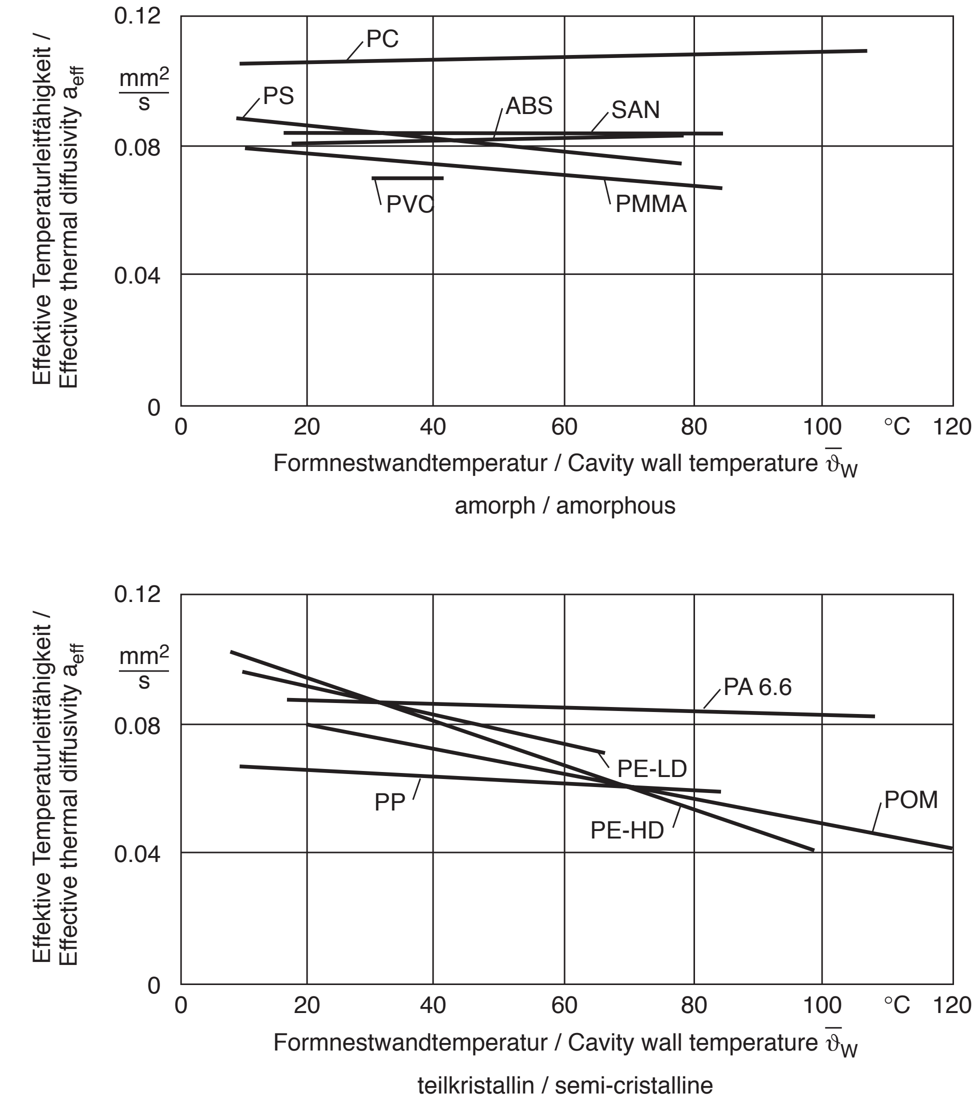

Fig. 17: Effective thermal diffusivity as a function of cavity wall temperature [7]

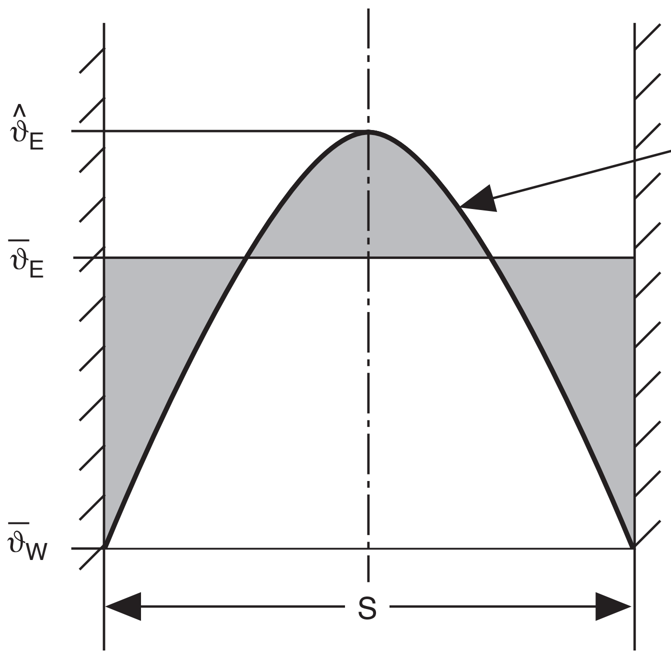

At the time of demolding a temperature profile has developed in the molding which can be characterized by

– the temperature in the centre of the molding $\hat{\vartheta}_E$
– the integral mean value over the cross-section $\overline{q}_E$.

Guide values for the demolding temperature can be taken from Fig. 1.

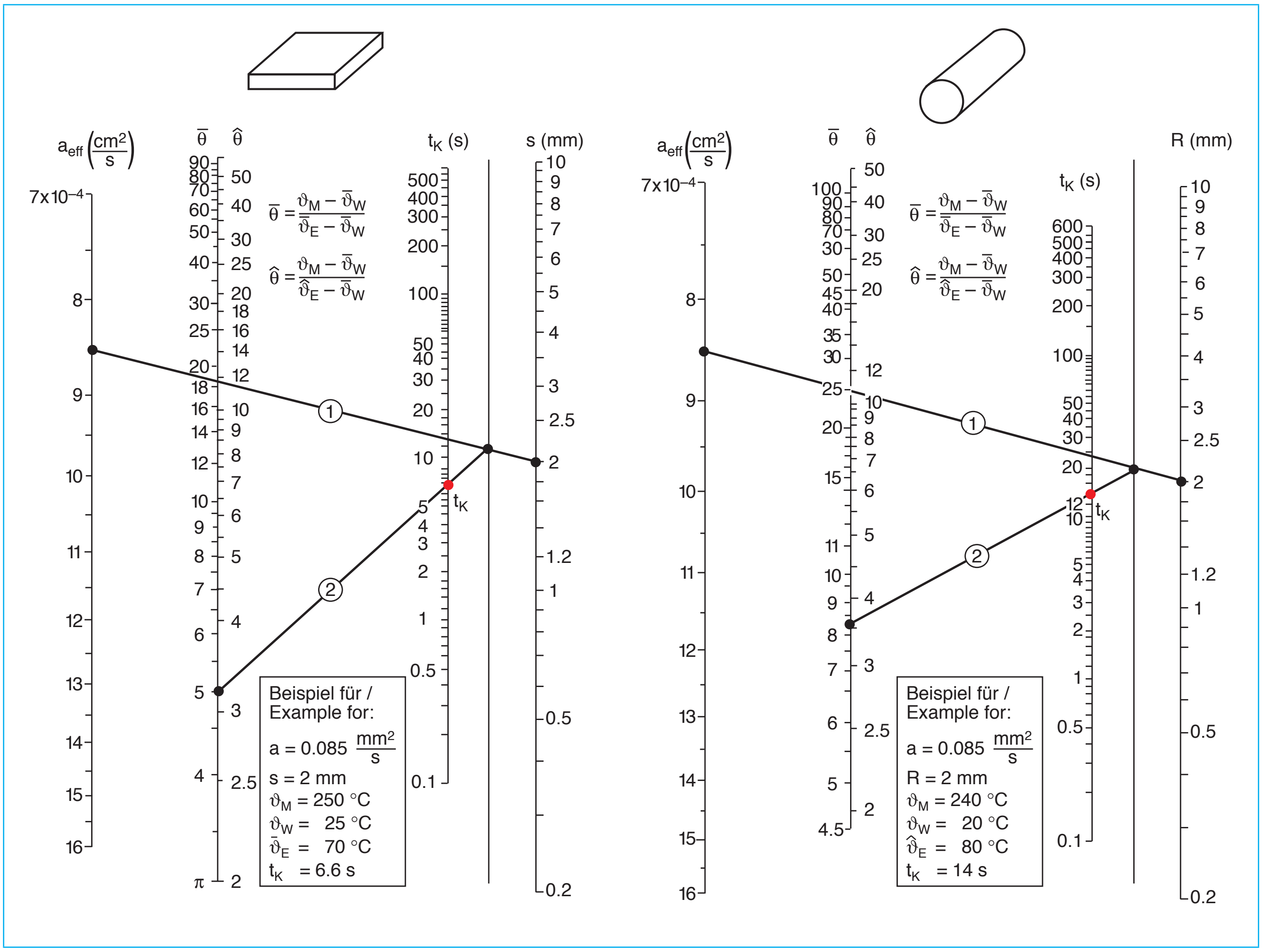

Fig. 18: Nomograms for determining the cooling time of plate-shaped (left) and cylindrical (right) molded parts [11]

The nomograms shown in Fig. 18 can additionally be used for purposes of estimating the cooling time. With knowledge of the material (a_{eff} = effective thermal diffusivity), the wall thickness s, and the degree of cooling U it is possible to establish the cooling time very rapidly in the manner set out above.

6.1 Selection of the geometry that dictates the cooling time

The design of the heating/cooling system should be based on the part of the molding or sprue region (cold runner) which needs to be cooled for longest before it can be demolded, i. e. until it has reached the permitted demolding temperature ϑ_E . Cold runner sprues do not always have to cool down to the point of dimensional stability but simply need to cool down far enough so as not to stick and cause marks (example: thin-walled molding with a thicker sprue).

If the sprue is not to dictate the cooling time under any circumstances, i. e. if the cooling time of the thicker area of the molding is to be greater than or equal to the cooling time of the sprue cross-section, then Equations 1 and 2 or 1a and 2a from Fig. 16 can be equated with each other:

Cooling $_{\text{timemolding}}$ ≥ cooling $_{\text{timesprue}}$

After the equation has been rewritten, the following relationship is obtained for the sprue diameter:

$$d_a = 1.53 \cdot s_{max} \sqrt{\frac{\ln\left[\frac{4}{\pi}\right] \cdot \theta}{\ln(1.599) \cdot \theta}}$$

$$\theta = \frac{T_M - \bar{T}_W}{\bar{T}_E - \bar{T}_W}$$

s_{max} = thickest part wall thickness
d_a = sprue diameter
a_{eff} = effective thermal diffusivity

6.2 Parameters influencing cooling time

If we observe the idealized and simplified equation for the cooling time of a flat plate (Equation 1 in Fig. 16)

$$t_K = \frac{s_{max}^2}{\pi^2 a_{eff}} \ln\left(\frac{4}{\pi} \cdot \theta\right)$$

$$\theta = \frac{T_M - \bar{T}_W}{\bar{T}_E - \bar{T}_W}$$

then there are four parameters which affect the cooling time (a_{eff}: quasi constant mean value from Fig. 17):

s^2 = square of molded part wall thickness
T_M = melt temperature after filling
$\overline{T}_E$ = mean demolding temperature
$\overline{T}_W$ = mean cavity wall temperature

It is the wall thickness (s^2!) that has by far the biggest influence on cooling time. Fig. 19 shows the correlation between the wall thickness (s) and the cooling time (t_K). The influence of the wall thickness is entered in squared form, which means that, if the wall thickness is doubled, this will lead to a fourfold increase in cooling time. This clearly highlights the conflict between a longer cooling and cycle time and the higher wall thickness which is frequently desirable in order to facilitate mold filling.

Fig. 20 shows the cooling time versus the demolding temperature of the molded part, with the molded part wall thickness as the parameter. Increasing the demolding temperature has the effect of reducing the cooling time. The upper limit for the demolding temperature is dictated by the degree of dimensional stability required. Shear modulus curves (shear modulus versus temperature) may be used here by way of an approximation.

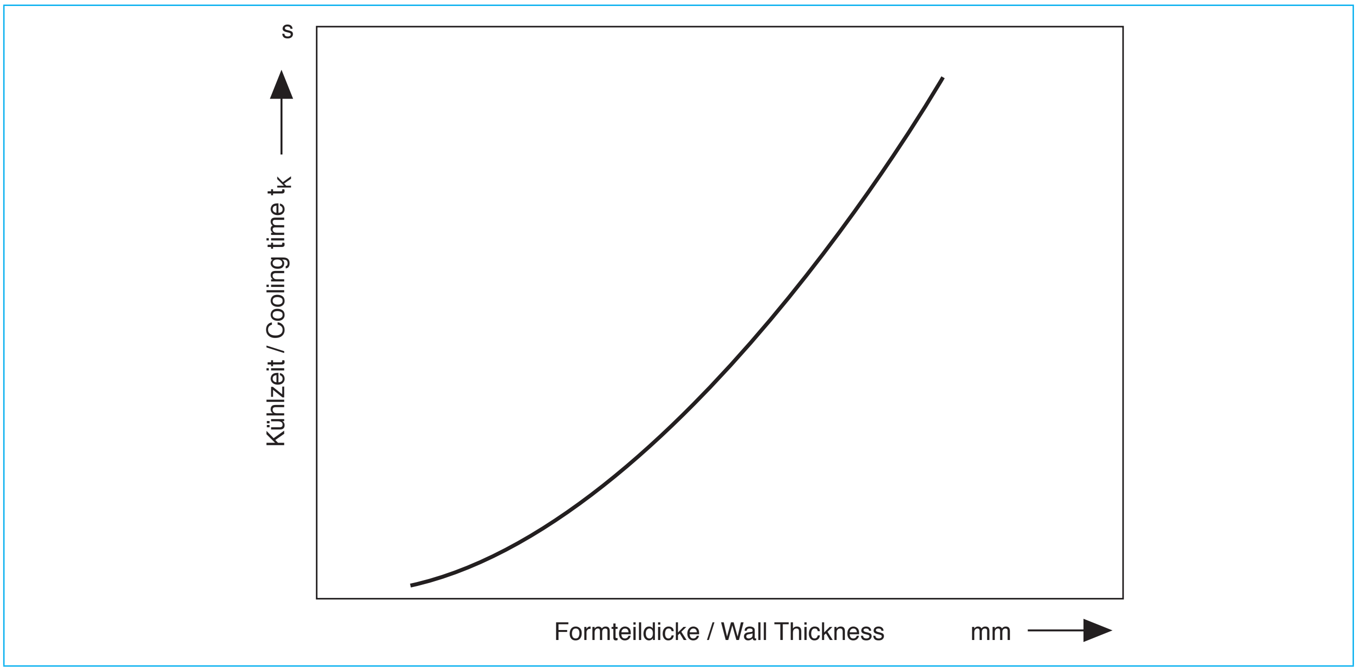

Fig. 19: Influence of wall thickness s on cooling time t_K

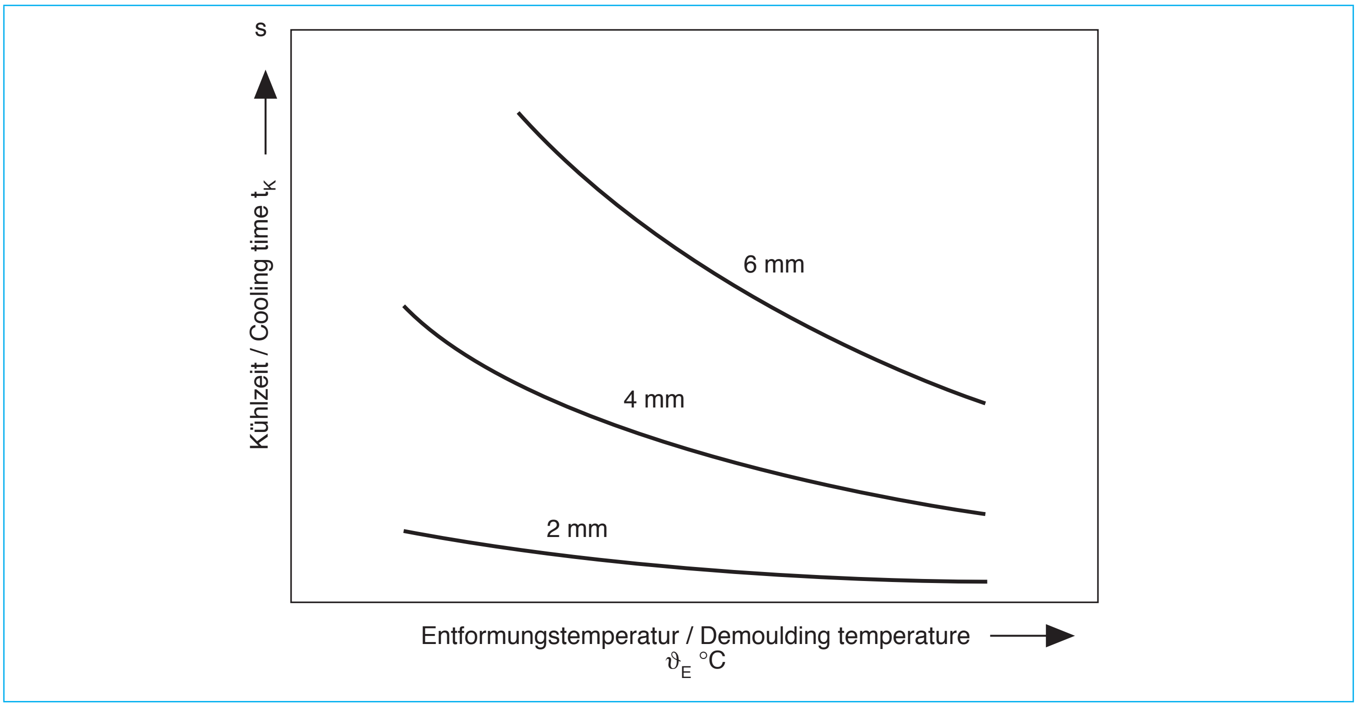

Fig. 20: Influence of demolding temperature on cooling time t_K

The cavity wall temperature has an inverse but no less pronounced influence on the cooling time (Fig. 21). An increase in the cooling time is observed when there is an increase in the cavity temperature.

The temperature of the melt has a very slight influence on the cooling time (Fig. 22). The cooling time increases slightly as the melt temperature rises. Even with large wall thicknesses, there is only a slight increase in the influence of melt temperature.

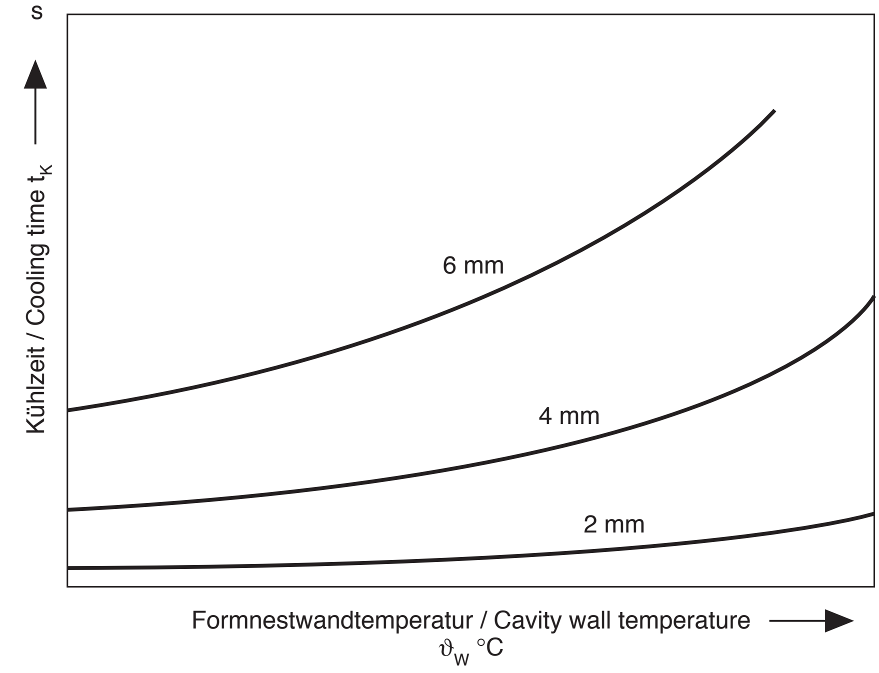

Fig. 21: Influence of cavity wall temperature on cooling time t_K

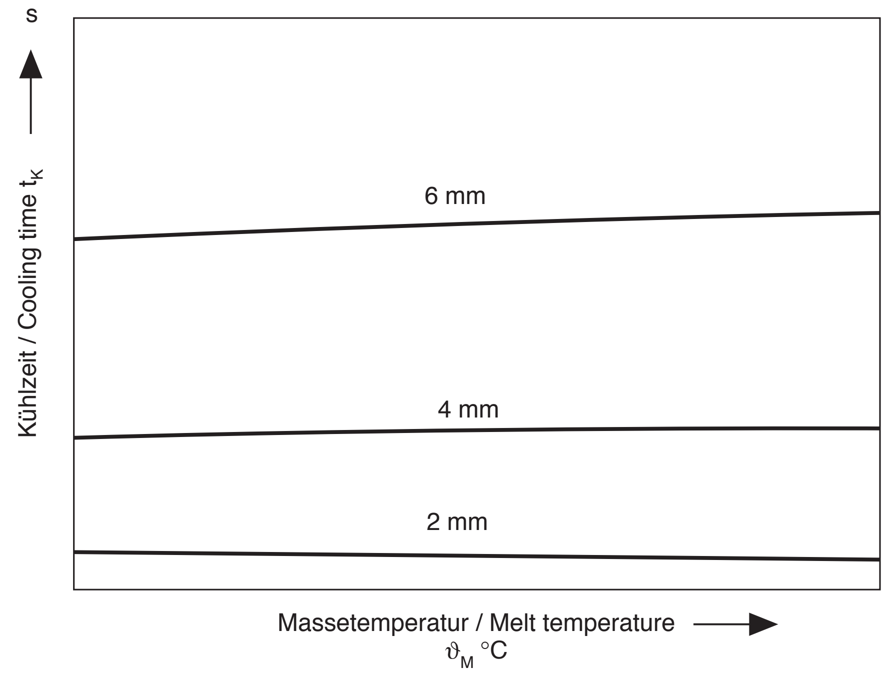

Fig. 22: Influence of melt temperature on cooling time t_K

The following points can be derived from what has been set out above:

– The molded part should not be any thicker than necessary. Partial increases in wall thickness should also be avoided if possible ($t_K \sim s^2$).
– To achieve a low cycle time, the demolding temperature should be selected as high as possible, although it is absolutely essential to pay attention to dimensional stability at the same time.
– It is important to select a reasonable mold temperature. (taking into account the raw materials manufacturer, the mechanical properties, matt or rough molding surfaces, gloss differences, stresses).
– Although the influence of the melt temperature is only low, it should not fall to too low a level in order to ensure better flowability of the melt.

7 Overall heat balance for the heating/cooling of the mold

The heat balance is drawn up by setting the flows of heat that are introduced into the mold against those that are removed from it. The individual heat flows are established in the form of mean values over an injection cycle and are regarded as stationary. The aim of the heat balance is to establish the quantity of heat that is to be eliminated by the heating/cooling medium (Fig. 23).

The heat balance for the entire mold is as follows:

$\dot{Q}_F$ = heat flow introduced into the mold by the hot molding compound
$\dot{Q}_L$ = heat flow given off to the surroundings by conduction
$\dot{Q}_K$ = heat flow given off to the surroundings by convection
$\dot{Q}_{Str}$ = heat flow given off by radiation
$\dot{Q}_{TM}$ = heat flow that the heating/cooling medium introduces or eliminates
$\dot{Q}_H$ = additional heat flow, such as through a hot runner block

In this balance, those heat flows that are introduced into the mold and thus heat it are counted as positive flows, while the heat flows that are removed from the mold, and thus cool it, are counted as negative.

When thermoplastics are being processed, the molding undergoes cooling, which is why $\dot{Q}_F$ is always positive, while the heat exchanged with the surroundings can be either positive or negative as a function of the temperature level of the mold. The same applies in the case of the heat flow for the heating/cooling medium, $\dot{Q}_{TM}$.

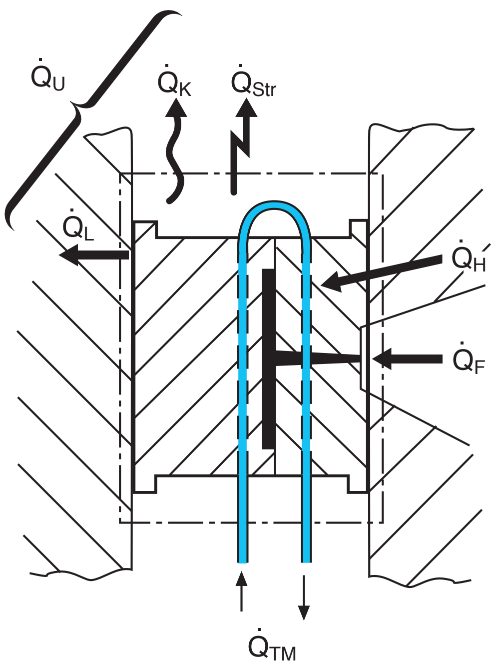

Fig. 23: Heat flow balance in an injection mold [7]

Heat flow of heating/cooling medium:

$$\dot{Q}_{TM} = \dot{Q}_F + \dot{Q}_H - \underbrace{(\dot{Q}_K + \dot{Q}_{Str} + \dot{Q}_L)}_{\text{Surroundings}}$$

In order to determine the heat of the molding ($\dot{Q}_F$), it is necessary to know the enthalpy differential (Δh) that prevails between the melt temperature ϑ_M and the demolding temperature ϑ_E. This can be obtained from enthalpy diagrams (Figs. 24 + 25) for the corresponding materials.

$$\dot{Q}_F = \frac{m \cdot \Delta h}{t}$$

m = molded part mass
t = cycle time
Δh = specific enthalpy differential

8 Heat exchange with the surroundings [7]

The heat exchange with the surroundings is very difficult to measure. In one study [7], component $\dot{Q}_U$ was determined indirectly with the machine running dry, i. e. without the molding compound being injected into the mold. In this case, the heat given off by the mold into the surroundings is equal to the heat taken up by the heating/cooling medium:

$$\Sigma_i \dot{Q}_i = 0$$
$$\dot{Q}_U = -\dot{Q}_{TM}$$

The measurements revealed a linear correlation between the heat exchange with the environment and the temperature of the heating/cooling medium. Direct proportionality is achieved if the quantity of heat $\dot{Q}_U$ is plotted against the temperature differential $\vartheta_{WA} - \vartheta_U$.

$$\dot{Q}_U \sim (\vartheta_{WA} - \vartheta_U)$$

ϑ_{WA} = temperature on the outer surface of the mold
ϑ_U = ambient temperature

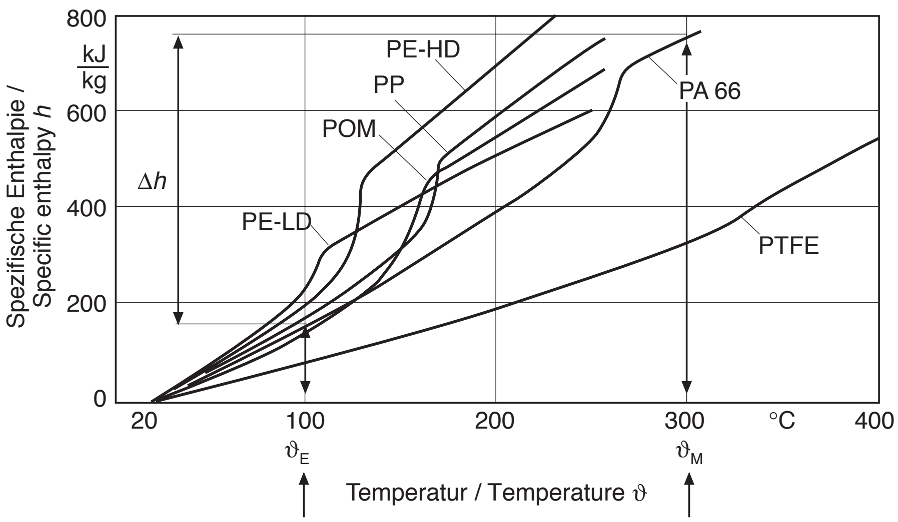

Fig. 24: Specific enthalpy for a number of semi-crystalline thermoplastics

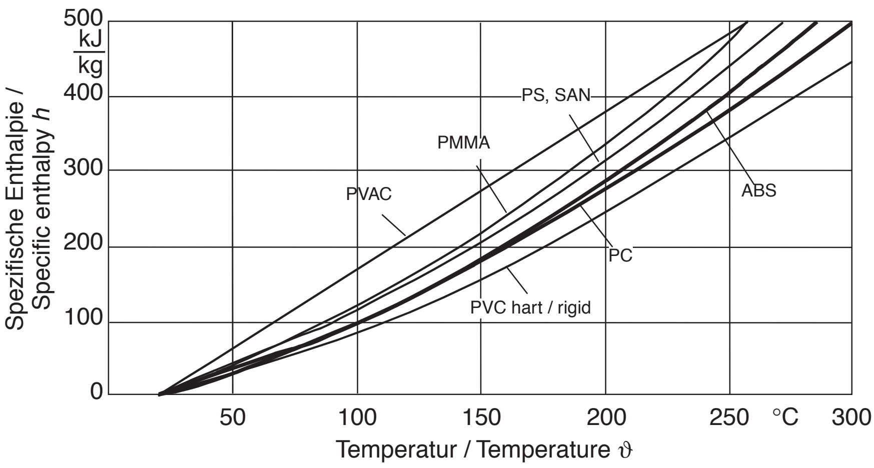

Fig. 25: Specific enthalpy for a number of amorphous thermoplastics [7]

Fig. 26 shows the heat exchange with the surroundings for three of the materials studied. The components accounted for by conduction, convection and radiation are indicated on the diagram.

8.1 Convection $\dot{Q}_K$

The convection component can be determined by Newton's law of heat transfer:

$$\dot{Q}_K = A_S \cdot \alpha_L (\vartheta_{WA} - \vartheta_U)$$

A_S = lateral side of mold
α_L = coefficient of heat transfer for natural convection in air
$\alpha_L \approx 8\ W/m^2 \cdot$ degree

The outside mold temperature is frequently unknown and can be determined from the following diagram (Fig. 27). This shows the measured correlation between the outside mold temperature and the heating/cooling medium temperature.

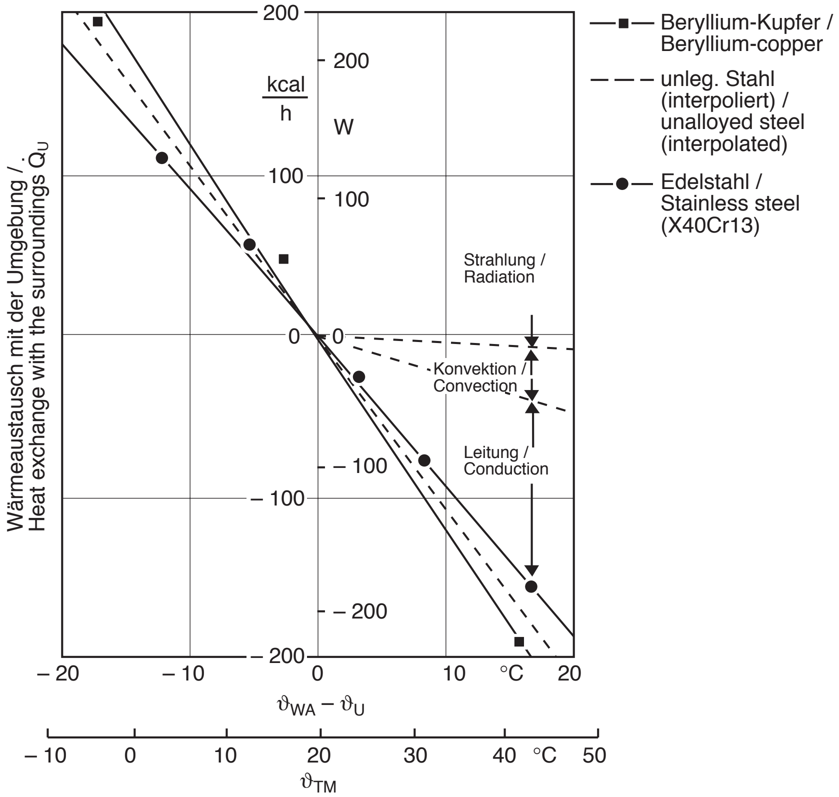

Fig. 26: Heat exchange between the mold and the surroundings with different heating/cooling medium temperatures [7]

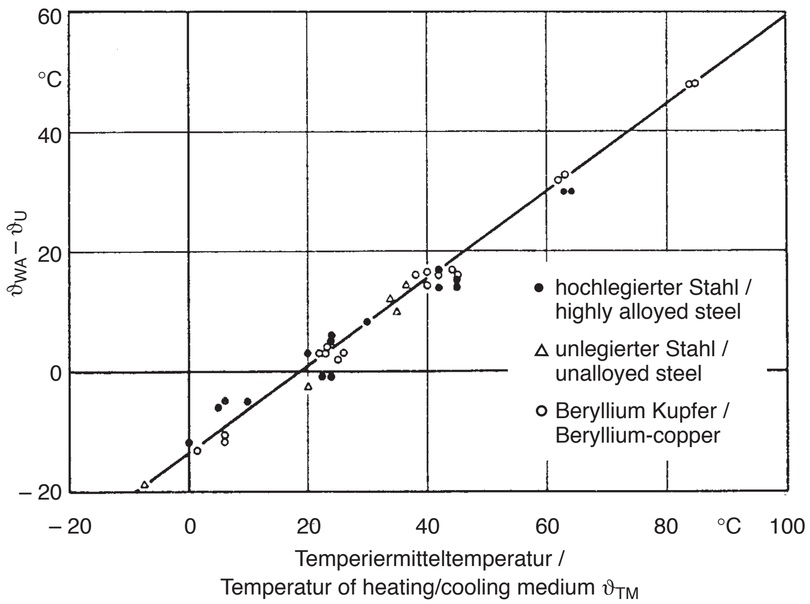

Fig. 27: Correlation between the temperature differential that prevails between the outside mold temperature ϑ_{WA} and the ambient temperature ϑ_U as well as the heating/cooling medium temperature [7]

If the exchange of heat with the surroundings via the parting plane is to be taken into account (when the mold is open), then the equation given for convection, $\dot{Q}_K$ should be supplemented by the factor:

$$A_{TR} \cdot \alpha_L (\vartheta_{WA} - \vartheta_U) \cdot \frac{t_{off}}{t_{Cycle}}$$

A_{TR} = parting plane
t_{off} = time for which the mold is open

Convection:

$$\dot{Q}_K = \alpha_L (\vartheta_{WA} - \vartheta_U) \cdot \left(A_S + \frac{A_{TR} \cdot t_{off}}{t_{Cycle}} \right)$$

$\dot{q}_K = \alpha_L (\vartheta_{WA} - \vartheta_U)$ = heat flow density

8.2 Radiation $\dot{Q}_{STR}$

The Stefan-Boltzmann law:

$$\dot{Q}_{Str} = A_S \cdot \varepsilon \cdot C_S \left[\left(\frac{T_{WA}}{100} \right)^4 - \left(\frac{T_U}{100} \right)^4 \right]$$

$$\dot{q}_{Str} = \varepsilon \cdot C_S \left[\left(\frac{T_{WA}}{100} \right)^4 - \left(\frac{T_U}{100} \right)^4 \right]$$

$\dot{q}_{Str}$ = heat flow density
A_S = lateral side of mold radiating heat
ε = emission factor ≈ 0.25 for brightly polished steel surface;
emission factor ≈ 0.8 for molds in production
C_S = radiation coefficient of the black body
T_{WA} = absolute outside mold temperature in K
T_U = absolute ambient temperature in K

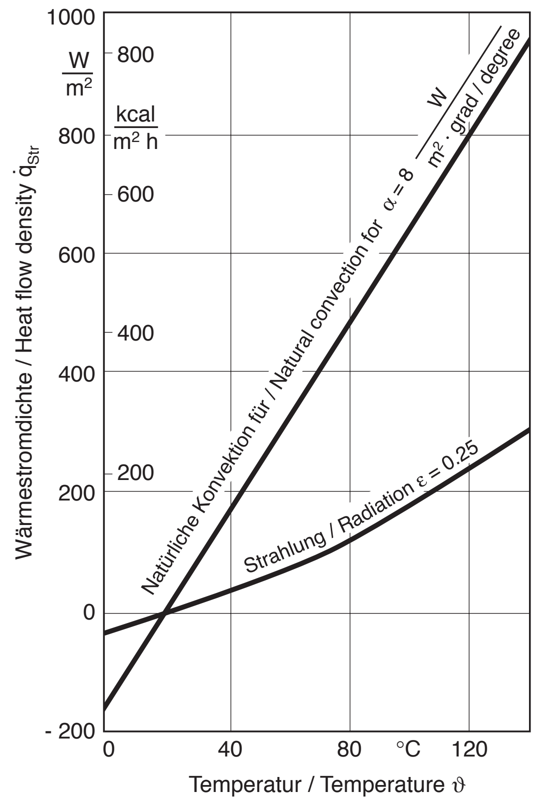

Fig. 28: Heat flow density for natural convection and radiation (ambient temperature ϑ_U = 20 °C) [7]

In the case of outside mold temperatures of up to 90 °C, the radiation component is less than 25 % of the convection component. Fig. 28 shows the equations for the two components in graph form. These can be used directly in mold design.

8.3 Conduction $\dot{Q}_L$

The conduction of heat in the platens can be expressed by the following equation:

$$\dot{Q}_L = A_A \cdot \beta \, (\vartheta_{WA} - \vartheta_U)$$

A_A = sum of both mold platens
β = coefficient of heat transfer

From the measurements in [7], we obtain the following values for the coefficient of heat transfer β.

β	Unalloyed steel	Highly alloyed steel	Copper alloys
$\frac{W}{m^2 \cdot degree}$	98	84	116

Table 2: Coefficient of heat transfer for different materials

The proportion of heat flow losses accounted for by conduction can be reduced by incorporating insulation between the mold and the platens. In this case, β is replaced by β_{isol}.

$$\beta_{isol} = \frac{\beta}{1 + \frac{s_{isol} \cdot \lambda_W}{l_F \cdot \lambda_{isol}}}$$

S_{isol} = thickness of insulation
l_F = pro rata mold height (≈ clamping height)
λ_W = thermal conductivity of mold
λ_{isol} = thermal conductivity of insulating plate

$$\lambda_{isol} \approx 0.7 \frac{W}{m \cdot K}$$

The heat exchange with the surroundings has now been fully recorded with the three heat components for the surroundings. If the temperature level of the mold deviates from the surrounding temperature by a pronounced margin, then the three components can assume considerable proportions. These must be taken into consideration with heating/cooling-medium temperatures of above 50 °C or so and of below 0 °C [7].

9 Temperature gradient from the cavity wall to the heating/cooling medium

Fig. 29 shows the temperature situation over the cross-section of the mold from the cavity wall to the cooling channel in qualitative terms. These are values that have been averaged out over time for a quasi-stationary machine operating state.

In order to ensure that the heating/cooling unit reacts as rapidly as possible to disturbances, the temperature differential between the cavity wall and the centre of the heating/cooling medium should be < 30 °C. This temperature differential is made up of two components:

– temperature differential due to heat conduction resistance $\Delta\vartheta_1$
– temperature differential due to heat transfer resistance $\Delta\vartheta_2$

The **temperature differential $\Delta\vartheta_1$** between the cavity surface and the cooling channel surface (heat conduction resistance) is affected by the thermal conductivity of the mold and the distance between the cooling channels. The following Figure makes it clear that the "heat conduction differential" is much lower for beryllium-copper than for a highly alloyed steel.

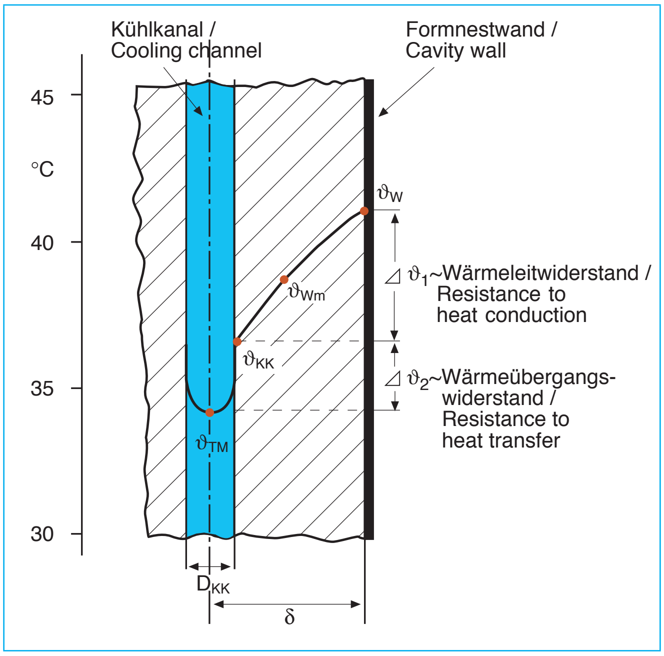

Fig. 29: Temperature profile from the cavity surface to the heating/cooling channel [7]

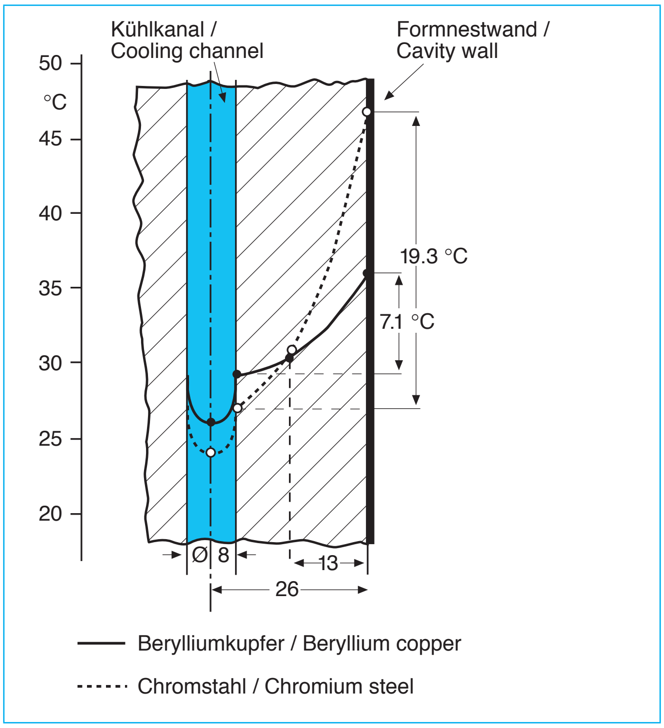

Fig. 30: Comparison of temperature profiles for different mold materials [7]

Temperature differential $\Delta\vartheta_2$ expresses the heat transfer from the mold material to the heating/cooling medium. $\Delta\vartheta_2$ represents the temperature differential between the wall of the cooling channel and the centre of the cooling channel. The level of this differential is determined by the heat transfer conditions to the heating/cooling medium.

Temperature differential $\Delta\vartheta_1$ (heat conduction) is always positive, while $\Delta\vartheta_2$ (heat transfer) can also assume negative values. This will be the case if the heat loss to the environment is greater than the heat input from the molding compound. In practice, this occurs when a high mold temperature level is employed (Fig. 31).

The coefficient of heat transfer α_{TM} (required to calculate $\Delta\vartheta_2$) can be calculated with the Hausen equation (Section 12.1). If water is used, then the coefficient of heat transfer can be read off directly from the following diagram.

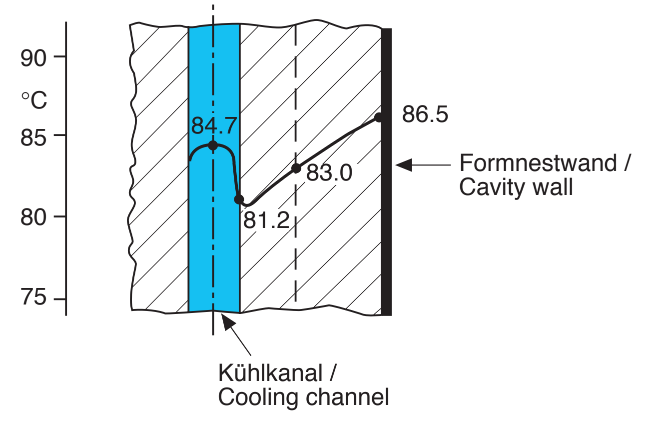

Fig. 31: Temperature profile in cavity with a high temperature level [7]

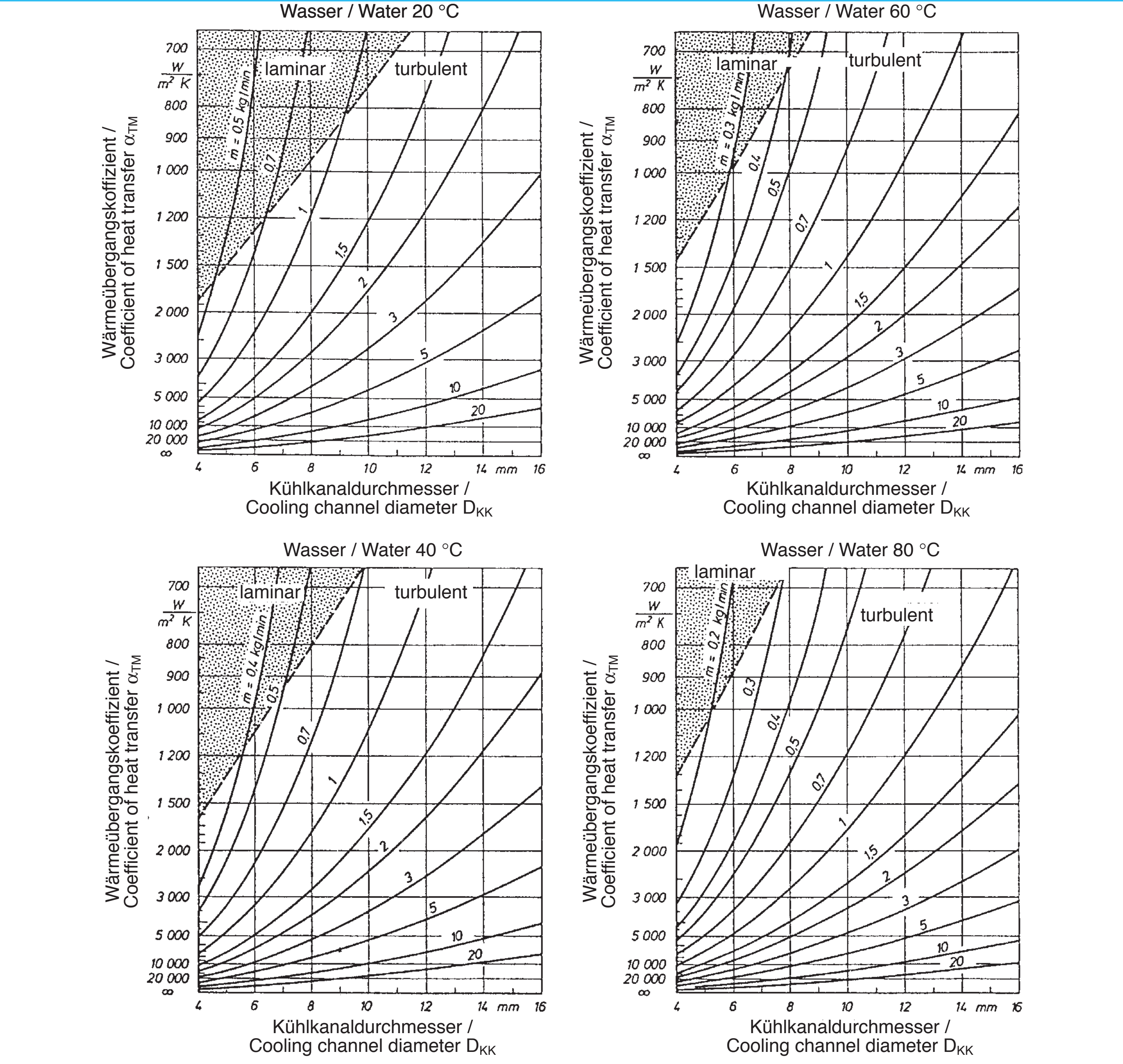

Fig. 32: Coefficient of heat transfer for water at different temperatures [12]

10 Position of the heating/cooling channels in relation to the cavity wall: heating/cooling error

The position of the heating/cooling channels is of decisive importance for uniform heating and cooling. In many cases, designers decide on the position of the heating/cooling channels as the last step of the mold design process before the mold is built. As a result, the heating/cooling channels are incorporated where there still happens to be space.

In the case of precision components, in particular, it is essential for the position of the heating/cooling channels to be included in the considerations for a new mold design right at the stage when the basic concept is being worked out. Allowance naturally has to be made for slides or bars, or other loose mold components, as well, but it is necessary to work out a compromize solution that guarantees optimum heating/cooling.

The ideal cooling situation in physical terms would be if individual heating/cooling channels of width b_T could heat/cool areas of the molding of width b_A. This state of affairs is shown in Fig. 33.

cool areas of the molding of width b_A. This state of affairs is shown in Fig. 33.

Rigidity problems can be expected with the shape that constitutes the ideal shape from the physical point of view.

By interrupting the channels of this shape, which has been optimized from the physical point of view, a sufficiently high rigidity can be achieved in the cavity to withstand the injection pressure (Fig. 34). This shape is used with heating/cooling channels that are helical, spiral or curved and to a lesser extent with ones that are straight. This shape requires an additional division of the mold platens and frequently involves elaborate milling and turning operations.

Heating/cooling channels with a circular cross-section are simpler to implement in technical terms (Fig. 35). These circular channels can be more readily integrated in the mold through drilling, and it is possible to avoid additional divisions in the mold platens, thereby ensuring a more rigid mold.

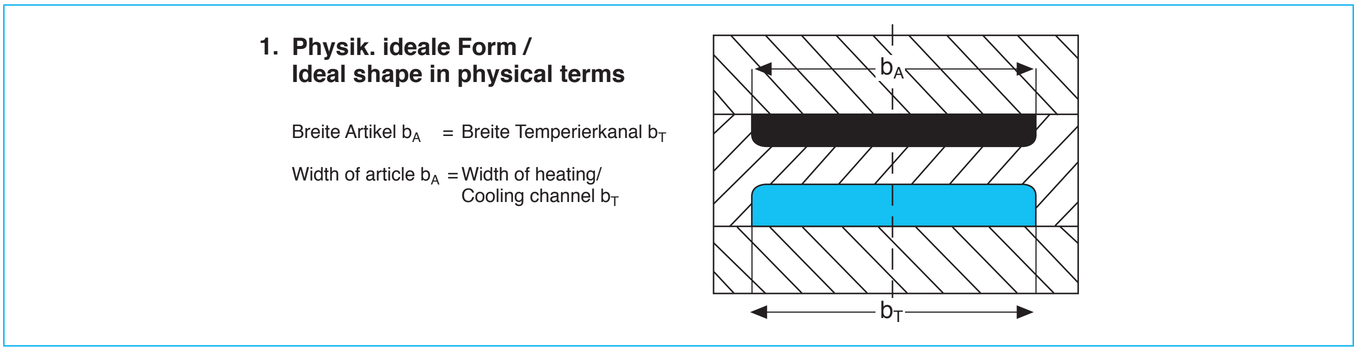

Fig. 33: Ideal shape of heating/cooling channel in physical terms [13]

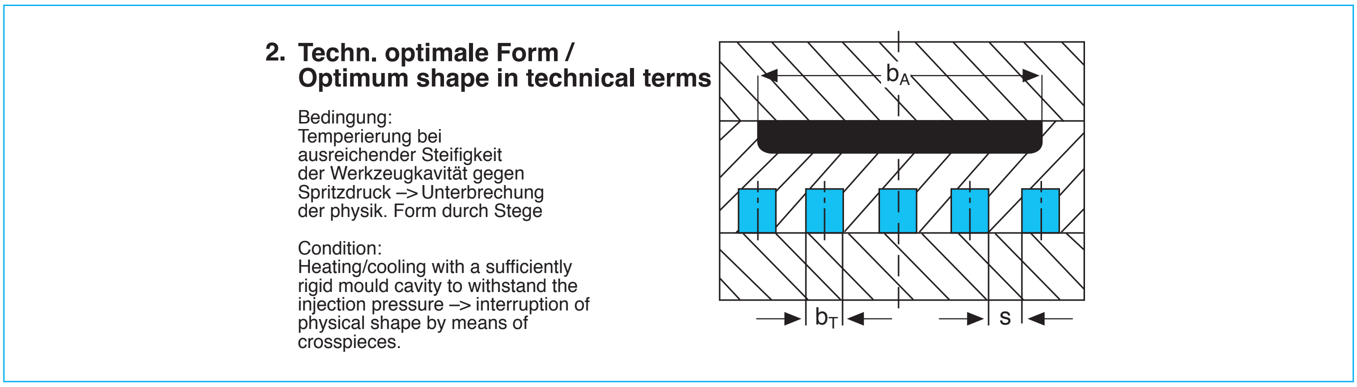

Fig. 34: Optimum shape of heating/cooling channel in technical terms [13]

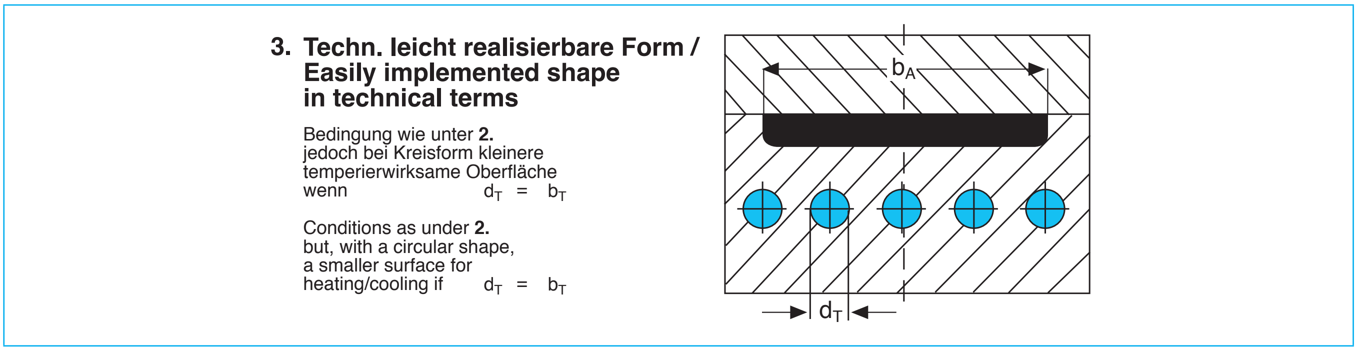

Fig. 35: Easy shape to manufacture [13]

Heating/cooling error

The position of the heating/cooling channels in relation to one another and in relation to the mold wall gives rise to a waveshaped temperature profile at the cavity wall, with a greater or lesser temperature differential $\Delta\vartheta_{Wij}$ on the mold wall (Fig. 36).

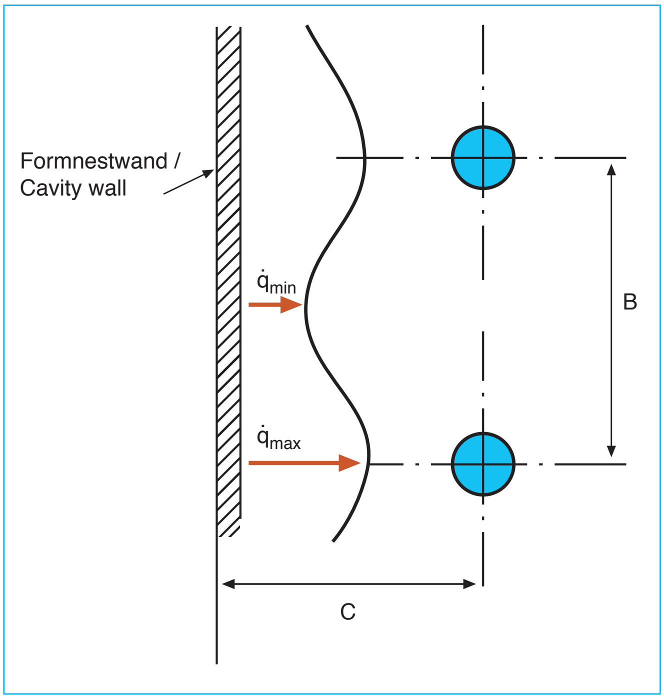

Fig. 36: Temperature profile at mold wall [14]

The temperature differential $\Delta\vartheta_{Wij}$ has nothing to do with the temperature fluctuations of a physical origin which occur at the cavity surface during the cycle (section 4). The homogeneity of the heating/cooling can be described on the basis of the heat flow profile (heat flow per area $\dot{q}$, Fig. 36). The areas of the molding that are positioned between the heating/cooling channels are not cooled as well ($\dot{q}_{min}$) as the areas located opposite the heating/cooling channel ($\dot{q}_{max}$). A bigger interval, B, will increase the difference between $\dot{q}_{min}$ and $\dot{q}_{max}$. A small interval, C, will similarly increase the difference. A greater or lesser "heating/cooling error" will result as a function of the particular combination of interval B and interval C. For reasons of homogeneity, this should not exceed

- 2.5 to 5 % for semi-crystalline thermoplastics

and

- 5 to 10 % for amorphous thermoplastics.

The heating/cooling error **j in %** works out at [14]

$$j = 2.4 \cdot Bi^{0.22} \cdot \left(\frac{B}{C}\right)^{2.8\left|\ln\left(\frac{B}{C}\right)\right|}$$

$$\text{with the Biot number: } Bi = \frac{\alpha_{TM} \cdot D_{KK}}{\lambda_W}$$

The heating/cooling error $\Delta\vartheta_{Wij}$ in °C for a medium cavity wall temperature is:

$$\Delta\vartheta_{Wij} = \bar{\vartheta}_W \cdot \frac{j}{100\ \%}$$

In theory, there are many different configurations that could be adopted for the heating/cooling channels. The different heating/cooling channel arrangements display different heat characteristics, however. Fig. 37 that follows shows a favorable and an unfavorable heating/cooling channel configuration.

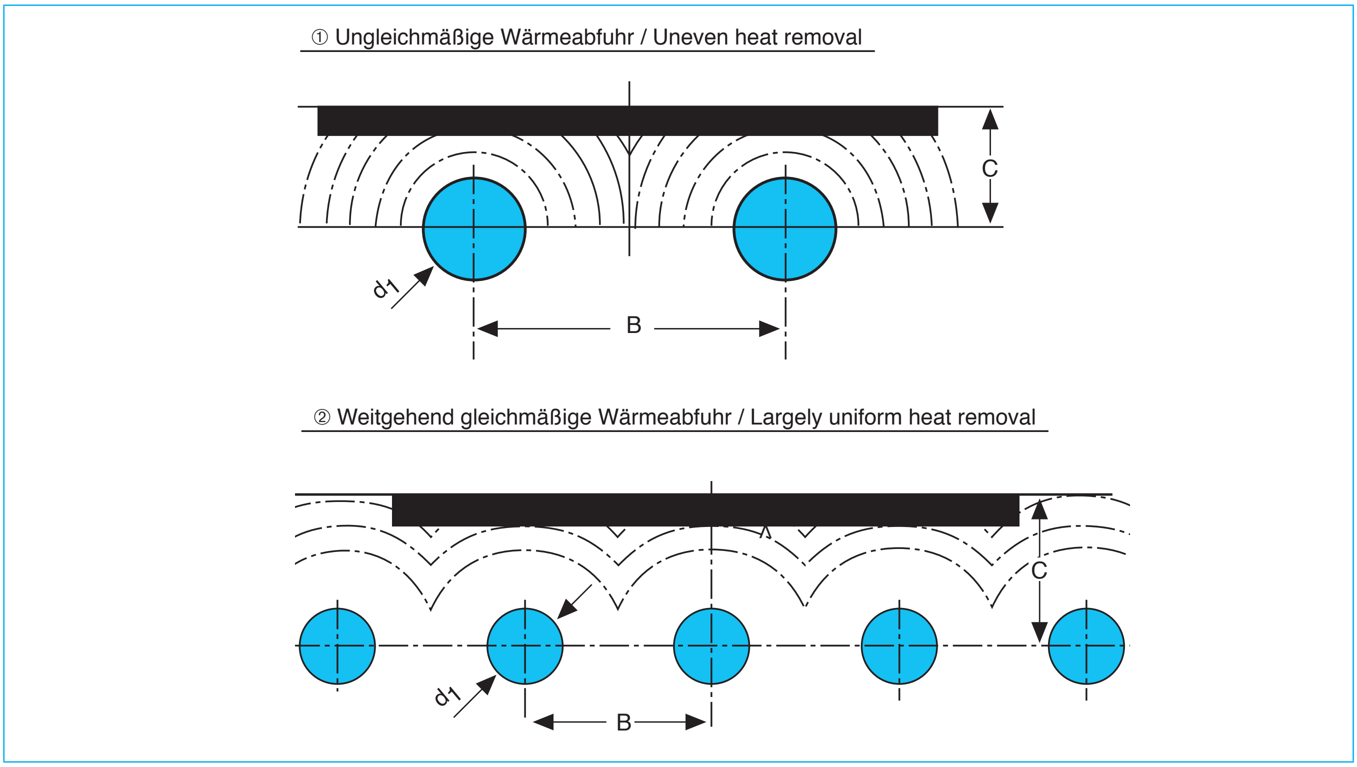

Fig. 37: Unfavorable and favorable design of heating/cooling channel

The uneven heating/cooling shown above is already evident from the heat flow profiles that are drawn in. The heating/cooling error, in %, will now be calculated as follows:

Example:

Heating/cooling medium throughput:	$\dot{m}_{TM} = 5 \frac{kg}{min}$
Heating/cooling medium:	**Water at 40 °C**
Coefficient of heat transfer:	α_{TM} : (Bild 32) $d_{T1} = 14$ mm -> $\alpha_{TM1} = 3000 \frac{W}{m^2 \cdot K}$ $d_{T2} = 9$ mm -> $\alpha_{TM2} = 7000 \frac{W}{m^2 \cdot K}$
Thermal conductivity of mould steel:	$\lambda_W = 30 \frac{W}{m^2 \cdot K}$
Moulded part thickness:	s = 3 mm

1. Uneven removal of heat

$d_{T1} = 14$ mm
$C_1 = 15$ mm
$B_1 = 35$ mm

Biot number:
Bi = 1.4

$$Bi = \frac{3000 \frac{W}{m^2 \cdot K} \cdot 0.014\ m}{30 \frac{W}{m \cdot K}}$$

Heating/cooling error j in %

$$j = 2.4 \cdot 1.4^{0.22} \left(\frac{35}{15}\right)^{2.8\left|\ln\left(\frac{35}{15}\right)\right|}$$

$$\underline{\underline{j = 19.3\ \%}}$$

2. Even removal of heat

$d_{T2} = 9$ mm
$C_2 = 24$ mm
$B_2 = 20$ mm

Biot number:
Bi = 2.1

$$Bi = \frac{7000 \frac{W}{m^2 \cdot K} \cdot 0.009\ m}{30 \frac{W}{m \cdot K}}$$

Heating/cooling error j in %

$$j = 2.4 \cdot 2.1^{0.22} \left(\frac{20}{24}\right)^{2.8\left|\ln\left(\frac{20}{24}\right)\right|}$$

$$\underline{\underline{j = 2.57\ \%}}$$

With a target mean mold surface temperature of $\overline{\vartheta}_W = 60\,°C$, the following mean temperature differential is obtained in °C:

uneven

$$\Delta\vartheta_{Wij} = 60\,°C \cdot \frac{19.3}{100}$$

$$\underline{\underline{\Delta\vartheta_{Wij} = 11.6\,°C}}$$

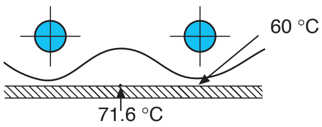

even

$$\Delta\vartheta_{Wij} = 60\,°C \cdot \frac{2.57}{100}$$

$$\underline{\underline{\Delta\vartheta_{Wij} = 1.54\,°C}}$$

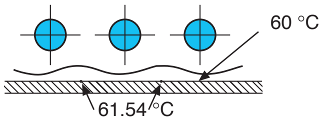

It can be seen from the calculation set out that, in the case of unfavorable heat removal, a temperature differential of 11 °C can be expected at the cavity surface.

In the case of uniform heat removal, there will be a percentage heating/cooling error within the ranges specified for semicrystalline and amorphous thermoplastics. The calculated temperature differential $\Delta\vartheta_{Wj}$ is also very low.

The example given shows how the heating/cooling channel layout can be verified for flat molded parts. For purposes of achieving uniform mold heating/cooling, the dimensions set out in Table 3 below have proved effective for the heating/cooling channel layout.

Wall thickness of injection molding part (mm)	Distance between centre of hole and injection molded part (mm)	Centreline spacing between holes (mm)	Hole diameter (mm)
0.0 to 1.0	11.3 to 15.0	10.0 to 13.0	4.5 to 6.0
1.0 to 2.0	15.0 to 21.0	13.0 to 19.0	6.0 to 8.5
2.0 to 4.0	21.0 to 27,.0	19.0 to 23.0	8.5 to 11.0
4.0 to 6.0	27.0 to 35.0	23.0 to 30.5	11.0 to 14.0
6.0 to 8.0	35.0 to 50.0	30.5 to 40.0	14.0 to 18.0

Table 3: Dimensions for the cooling channel geometry [15]

In contrast to the cooling of flat moldings, where uniform cooling can be achieved through the combination of channel position and diameter as shown, when it comes to cooling small-diameter cores, problems are encountered in removing the heat in an appropriate manner at all.

In almost all cases, the molding compound shrinks on to the core once it has been injected into the cavity and thus ensures a direct transfer of heat to the core. A gap develops between the molding compound and the mold, with heat being conducted less well over this gap. The biggest quantity of heat is transferred to the core. With long, thin cores, in particular, it is then possible for thermal loading to occur. This can increase the cycle time or even bring production to a standstill. Fig. 38 below contains suggested designs for the cooling of long cores with small diameters or widths..

Core diameter core width d (mm)	Description	Design
≥ 3	Heat elimination by air with open mold	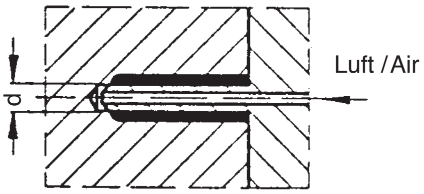
≥ 5	Copper or thermally conductive pipe to conduct heat to the heating/cooling medium	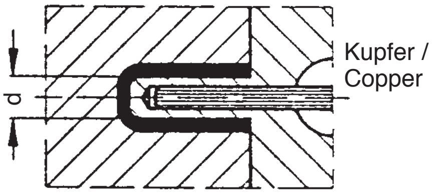
≥ 8	Long slender heating	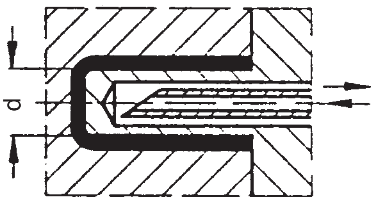
≥ 40	Spiral heating/cooling channel	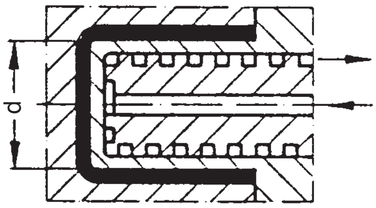
Pipe core s ≥ 4	Heating/cooling for pipe core with a double flighted spiral	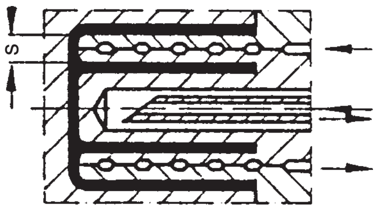

Fig. 38: Heating/cooling systems for cores [13]

In many cases, the make-up of the mold (slide bars, ejectors, runner system, etc.) makes it impossible for the design engineer to select an optimum position for cooling channels created by the conventional drilling method.

With small and medium-sized molds, in particular, special bonding techniques will nonetheless still permit optimum positioning of the cooling channels. This technique involves the mold inserts or the cores being designed so that they are separated in the cooling channel plane. The channels are then worked into the mold, being "simply" routed round other parts of the mold. The separated inserts are joined together under a vacuum by special bonding techniques. The inserts or cores are then ground to the right dimensions. Fig. 39 illustrates this technique on a flat molding, while Fig. 40 shows an application with core cooling.

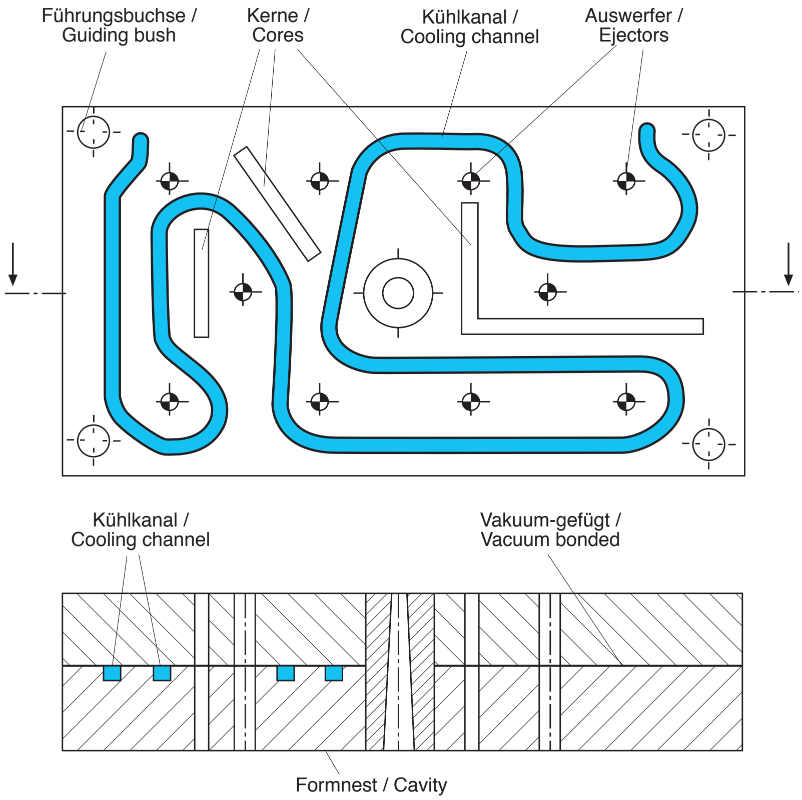

Fig. 39: Optimized position of the heating/cooling channels through joined mold plates

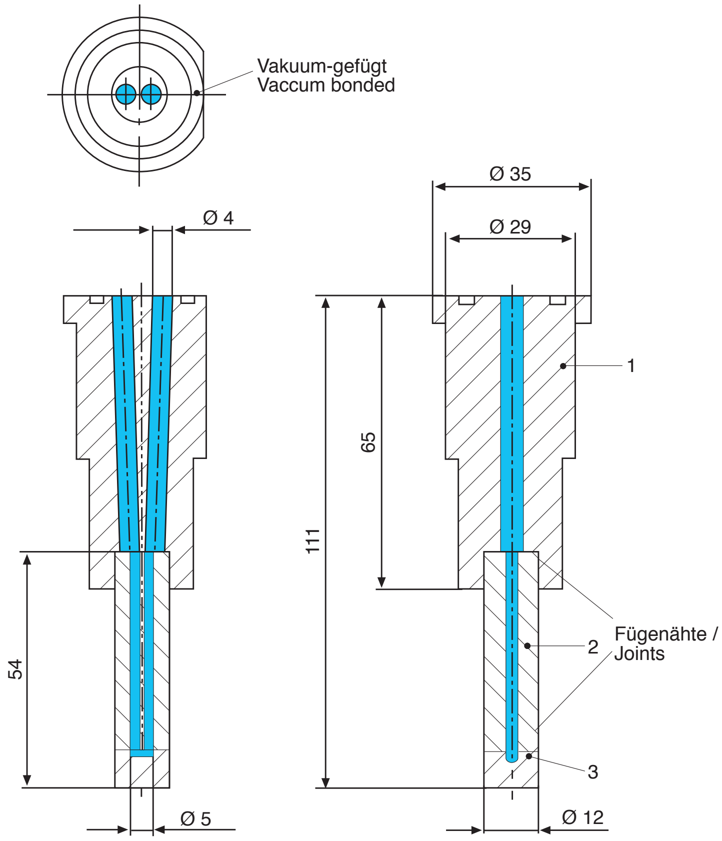

Fig. 40: Optimized heating/cooling system for cores employing the joining technique; source: Innova Engineering/System CONTURA®

11 Pressure losses in the heating/cooling system

Once the layout of the heating/cooling channel has been determined, the pressure losses and requisite pump capacity can be calculated. Allowance must also be made here for pressure losses incurred through flow deflections and flow junctions. The necessary pump capacity can then be established from the sum of all the pressure losses.

The pressure losses can be reduced through a parallel configuration of heating/cooling channels. Care should, however, be taken to ensure that the same pressure losses prevail in channel sections lined up in parallel (identical lengths and diameters).

In many cases, the pump on the heating/cooling unit does not supply the pressure necessary to ensure a sufficient throughput of heating/cooling medium (10 to 15 l/min), or a pressure-limiting valve dictates a very low maximum pressure level (Fig. 42). This results in a “creeping flow” (no turbulence) and hence an inadequate heat exchange inside the mold. The temperature differential between the inflow and outflow for the heating/cooling unit can indicate when there is an excessively low throughput: this should be < 4 °C (< 2 °C for precision moldings).

$$\Delta p_{KK} = \zeta \cdot \frac{l_{TK}}{D_{KK}} \cdot \frac{\rho_{TM}}{2} \cdot v_{TM}^2 \quad \text{(Round heating cooling channel)}$$

$$\zeta = \frac{0.316}{Re^{0.25}} \quad (2320 < Re < 100\,000)$$

$$\Delta p_{KN} = n_{KN} \cdot \zeta_{KN} \cdot \frac{\rho_{TM}}{2} \cdot v_{TM}^2 \quad \text{(Sharp-edged 90° bend)}$$

$$\Delta p_{Bo} = n_{Bo} \cdot \zeta_{Bo} \cdot \frac{\rho_{TM}}{2} \cdot v_{TM}^2 \quad \text{(Round 90° curve)}$$

$$\Delta p_{\text{Junctions}} \quad \text{(Pressure loss at junctions)}$$

$$\Delta p_{ges} = \Delta p_{KK} + \Delta p_{KN} + \Delta p_{Bo} + \Delta p_{A:\ \text{Junctions}}$$

$$N_p = \frac{\dot{m}_{TM}}{\rho_{TM}} \cdot \Delta p_{ges} \quad \text{Pump capacity}$$

Fig. 41: Pressure losses and requisite pump capacity

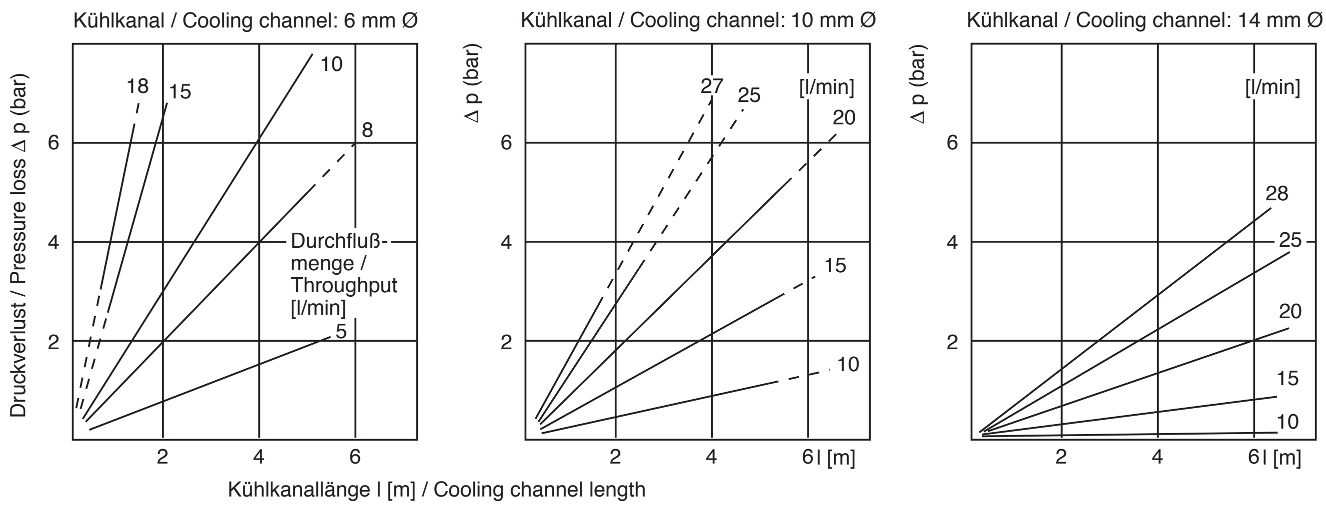

Fig. 42: Pressure loss measured in heating/cooling channels of different diameters [6]

12 Calculation methods for thermal mold design

The preceding sections have set out key theoretical correlations and design steps for the thermal design of the mold.

To sum up, a list is given here of the characteristic values that the design engineer ought to calculate when establishing the thermal layout of the mold:

- cooling and cycle time
- heat flows
- temperature profile in molded part and mold
- position and size of heating/cooling channels
- throughput and temperature of heating/cooling medium
- temperature homogeneity or temperature error at cavity wall
- pumping, cooling and heating capacity of heating/cooling unit (pressure losses in heating/cooling channels)
- simulation and variation of parameters (temperatures, material, processing parameters)

Three calculation methods are available for this:

12.1 Balance space method

The stages involved in design by the balance space method are essentially based on the correlations set out in the preceding sections.

The aids employed here (analytic equations, nomograms, diagrams) are derived from simplifications of the complex temperature processes. The idealized assumptions include:

- unidimensional heat flows
- neglection of start-up processes
- constant mean values over time (quasi-stationary state, i.e. regular temperature fluctuations are neglected)

As the name of this method suggests, a balance is drawn up of the heat flows within a balance space, i.e. in the mold. This balance space generally includes both halves of the mold and the entire molded part. It may, however, take in just one half of the molded part and the mold. Fig. 43 shows a flow diagram of the individual steps in the balance space method.

As the first step, the balance space under observation is determined. The minimum cooling time is calculated on the basis of the molded part geometry. The heat introduced into the mold has to be eliminated within the cycle time (cooling time + ancillary time). The heat flow that needs to be eliminated by the cooling medium is then established through the heat flow balance.

This is followed by the calculation of the throughput for the heating/cooling medium and the specification of the heating/cooling channel diameter. The heating/cooling error is obtained from the provisionally specified position of the channels both in relation to each other and in relation to the cavity wall. This error may necessitate a new channel layout. The pressure loss in the heating/cooling channels is calculated as the final step.

The equations required for the individual steps of the balance space method are set out below.

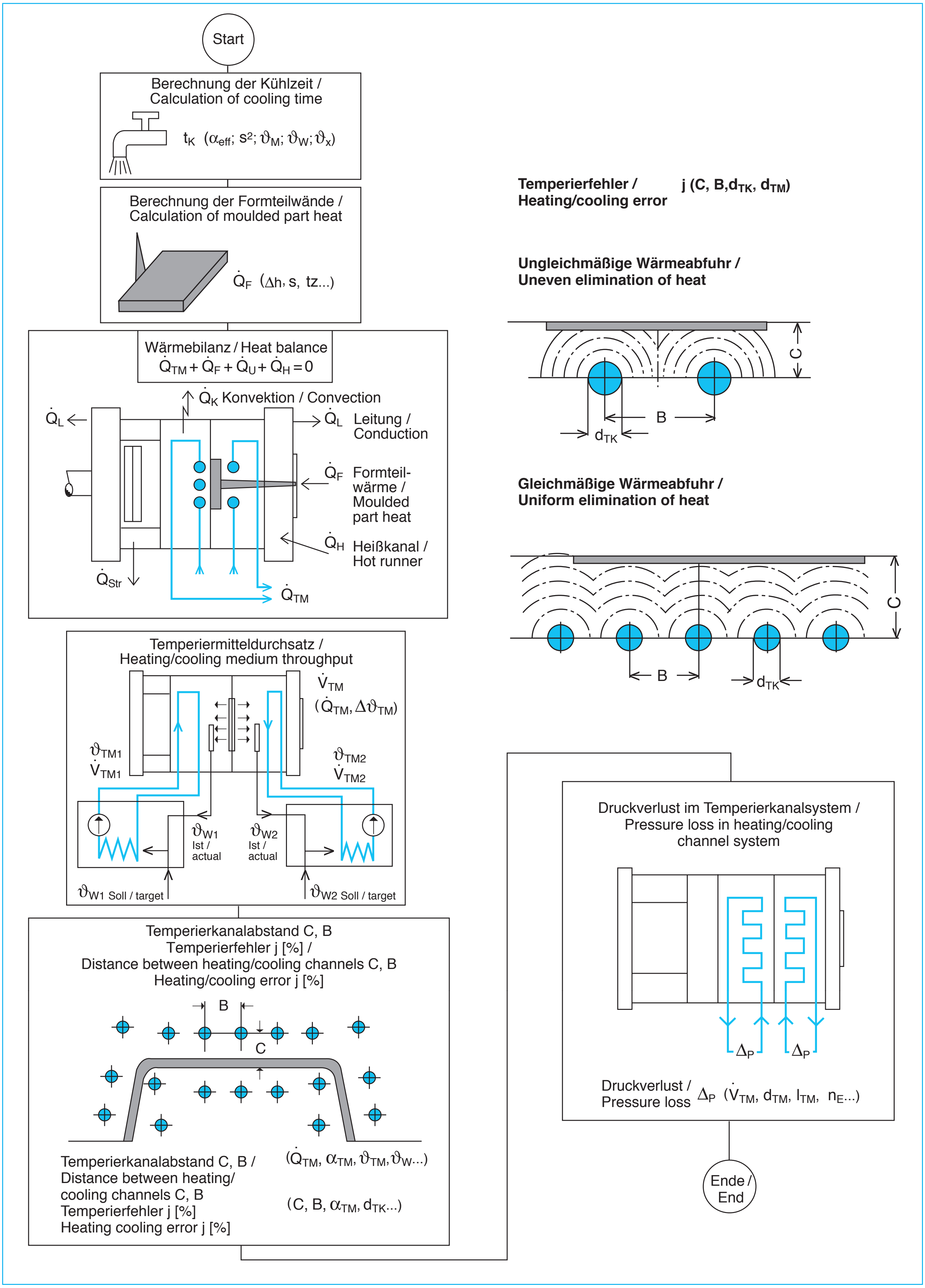

Fig. 43: Individual stages of thermal design by the balance space method

Equations for the design stages

<table>
<tr><td>1. Cooling time calculation</td><td>(see page 16, cooling time equations)</td></tr>
<tr><td>2. Heat flows
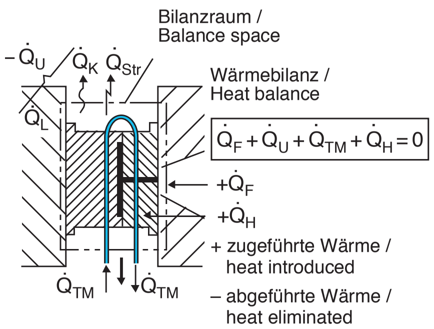</td><td>$\dot{Q}_F + \dot{Q}_{TM} + \dot{Q}_L + \dot{Q}_K + \dot{Q}_{Str} + \dot{Q}_H = 0$ with $\dot{Q}_L + \dot{Q}_K + \dot{Q}_{Str} = \dot{Q}_U$ (Heat flow to the surroundings)

Plastic: $\dot{Q}_F = \frac{m \cdot (h_1 - h_2)}{t_{Zyklus / Cycle}}$

Radiation: $\dot{Q}_{Str} = A_S \cdot \dot{q}_{Str} + A_{TR} \cdot \dot{q}_{Str} \cdot \frac{t_{off}}{t_{Zyklus / Cycle}}$

$\dot{q}_{Str} = \varepsilon \cdot C_S \cdot \left[\left[\frac{T_{WA}}{100}\right]^4 - \left[\frac{T_U}{100}\right]^4\right]$

Convection: $\dot{Q}_K = A_S \cdot \dot{q}_K + A_{TR} \cdot \dot{q}_K \cdot \frac{t_{off}}{t_{Zyklus / Cycle}}$

$\dot{q}_K = \alpha_L \cdot (\vartheta_{WA} - \vartheta_U)$

Conduction: $\dot{Q}_L = A_A \cdot \beta \cdot (\vartheta_{WA} - \vartheta_U)$

Insulation: $\beta_{isol} = \frac{\beta}{\frac{s_{isol} \cdot \lambda_W}{l_F \cdot \lambda_{isol}}}$</td></tr>
<tr><td>3. Heating/cooling medium throughput
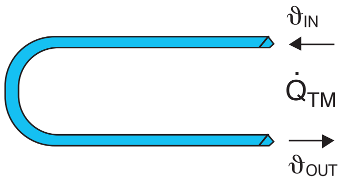</td><td>When the heat flows have been established, the amount of heat to be eliminated or introduced by the heating/cooling medium is known

$\dot{Q}_F + \dot{Q}_H - \dot{Q}_U$ $\quad \dot{Q}_{TM} = \dot{m}_{TM} \cdot c_{TM} \cdot (\vartheta_{IN} - \vartheta_{OUT})$

bzw. $\dot{m}_{TM} = \frac{\dot{Q}_{TM}}{c_{TM} \cdot (\vartheta_{IN} - \vartheta_{OUT})}$

$(\vartheta_{IN} - \vartheta_{OUT}) < 2$ °C für Präzisionsspritzteile / for precision injection mouldings</td></tr>
<tr><td>4. Diameter of heating/cooling channel
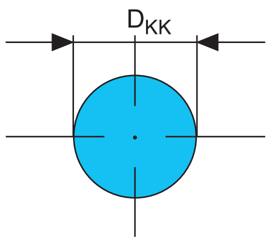</td><td>Condition: turbulent flow => Reynolds number much greater than 2300

$Re = \frac{v_{TM} \cdot D_{KK}}{\nu_{TM}} \gg 2\,300$ (dimensionslos / dimensionless) mit $v_{TM} = \frac{4 \cdot \dot{m}_{PU}}{\pi \cdot D^2_{KK} \cdot \rho_{TM}}$

with a non-circular channel cross-section: hydraulic diameter (A: cross-section; U = circumference) $D_{HY} = \frac{4 \cdot A}{U}$</td></tr>
</table>

5. Position of temperature channels and temperature gradient from the cavity wall

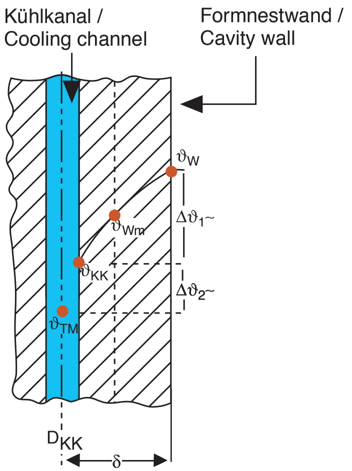

$\Delta\vartheta_1 = \vartheta_W - \vartheta_{KK}$ ~ Resistance to heat conduction

$\Delta\vartheta_2 = \vartheta_{KK} - \vartheta_{TM}$ ~ Resistance to heat transfer

$$\Delta\vartheta_1 = \vartheta_W - \vartheta_{KK} = \frac{\dot{Q}_F \cdot \delta \cdot n_{FT}}{2 \cdot A_F \cdot \lambda_W}$$

$$\Delta\vartheta_2 = \vartheta_{KK} - \vartheta_{TM} = \frac{\dot{Q}_F + \dot{Q}_U + \dot{Q}_H}{2 \cdot A_{KK} \cdot \alpha_{TM}}$$

Coefficient of heat transfer α_{TM}

$$\alpha_{TM} = \frac{Nu \cdot \lambda_{TM}}{D_{KK}}$$

Nusselt number::

$$Nu = 0.037 \cdot (Re^{0.75} - 180) \cdot Pr^{0.42} \cdot (1 + \left[\frac{D_{KK}}{l_{TK}}\right]^{0.67})$$

Valid for (Re < 106) and (0.6 < Pr < 500)

Reynolds number:

$$Re = \frac{v_{TM} \cdot D_{KK}}{\nu_{TM}} = \frac{v_{TM} \cdot D_{KK} \cdot \rho_{TM}}{\eta_{TM}}$$

Prandtl number:

$$Pr = \frac{\nu_{TM}}{a_{TM}}$$

Thermal conductivity:

$$a_{TM} = \frac{\lambda_{TM}}{c_{TM} \cdot \rho_{TM}}$$

$$\vartheta_{TM} = \vartheta_W - \Delta\vartheta_1 - \Delta\vartheta_2$$

$$\vartheta_W = \vartheta_{TM} + \Delta\vartheta_1 + \Delta\vartheta_2$$

If the temperature of the heating/cooling medium is specified, then the resultant mold wall temperature (cavity wall temperature) ϑ_W can be determined instead.

6. Heating/cooling errors

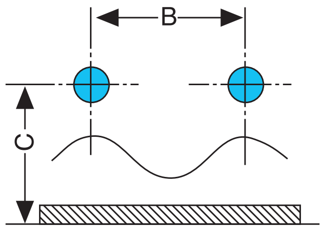

$$j = 2.4 \cdot Bi^{0.22} \cdot \left(\frac{B}{C}\right)^{2.8 \cdot \left|\ln\left(\frac{B}{C}\right)\right|}$$ in (%)

$$\Delta\vartheta_{Wij} = \bar{\vartheta}_W \cdot \frac{j}{100\ \%}$$ in (°C)

with the Biot number

$$Bi = \frac{\alpha_{TM} \cdot D_{KK}}{\lambda_W}$$

2.5 – 5 % for semi-crystalline thermoplastics
5 – 10 % for amorphous thermoplastics

7. Pressure losses in the heating/cooling system Pump capacity	$\Delta p_{KK} = \zeta \cdot \frac{l_{TK} \cdot \rho_{TM}}{2 \cdot D_{KK}} \cdot v^2_{TM}$	$\zeta = \frac{0.316}{Re^{0.25}}$ (Coefficient of friction)
	$\Delta p_{kN} = n_{KN} \cdot \zeta_{KN} \cdot \frac{\rho_{TM}}{2} \cdot v^2_{TM}$	Pressure loss, sharp-edged 90° bend
	$\Delta p_{B\sigma} = n_{B\sigma} \cdot \zeta_{B\sigma} \cdot \frac{\rho_{TM}}{2} \cdot v^2_{TM}$	(Pressure loss, round 90° curve)
	$\Delta p_{ges/tot} = \Delta p_{KK} + \Delta p_{KN} + \Delta p_{B\sigma}$	Pump capacity: $N_p = \frac{\dot{m}_{TM}}{\rho_{TM}} \cdot \Delta p_{ges/tot}$
8. Verification	Since the temperature of the heating/cooling medium ϑ_{TM} has so far been included in the calculation, a check is now conducted on this temperature. If the difference between the calculated temperature ϑ_{TM2} and the specified temperature ϑ_{TM1} is less than 2 °C, the calculation can be terminated. If the difference is more than 2 °C, ϑ_{TM2} must be taken as the starting value for a new calculation.	

12.2 Segmented design of heating/cooling system

After the initial rough dimensioning, the design of the heating/ cooling system can be worked out in detail. It is now established which areas of the molded part are to be cooled by which cooling elements.

The design of a segmented heating/cooling system is carried out in two stages:

1. Calculation of the heat conduction resistance of the cooling segment (geometry of the relevant area of the molded part).

   For a large number of heating/cooling elements, the calculation of the heat conduction resistance, WLW, is reduced to the calculation of a flat plate or a rectangular sleeve, cooled by a round cooling element. Since cooling takes place on both sides, only half the molding thickness is taken into account for the area of the molding under consideration.

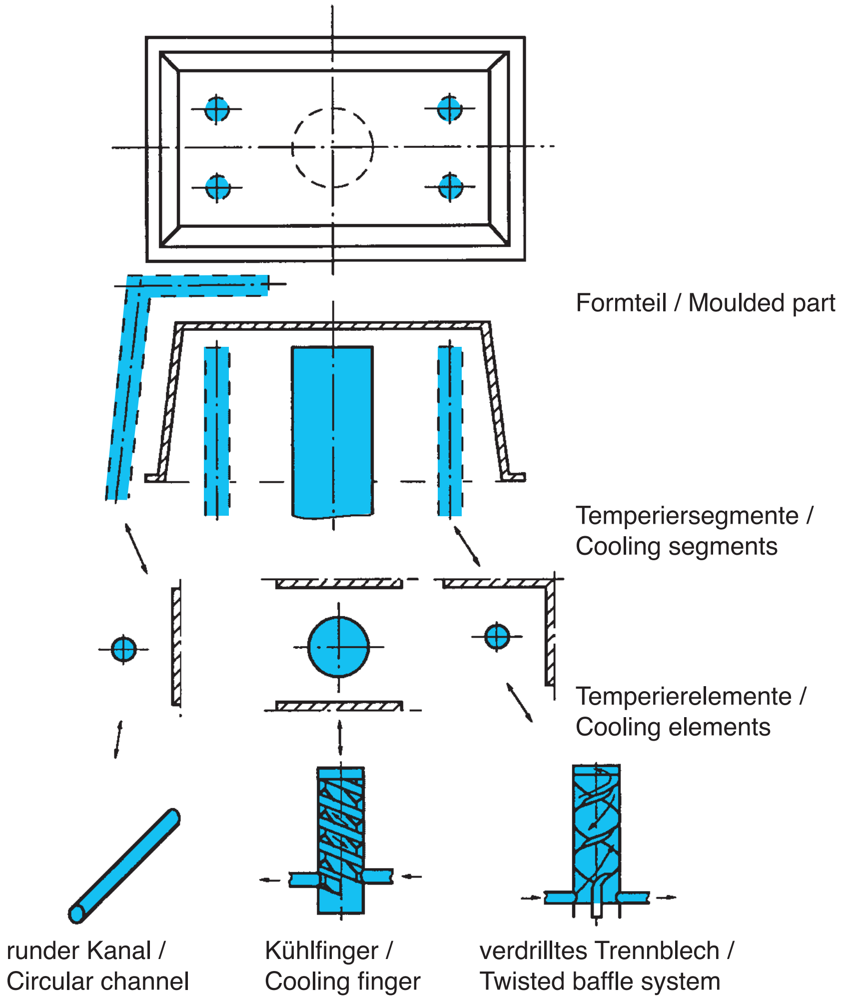

Fig. 44: The segmented cooling system method [10]

Grundgleichungen / Basic equations

$$\dot{Q}_{FTS} = \frac{\Delta h \cdot \varphi}{t_K + t_N} \cdot L \cdot b \, \frac{s}{2} \cdot \boxed{K_1}$$

$$WLW = \frac{1}{2 \cdot \pi \cdot L \cdot \lambda_N} \cdot \ln\left[\frac{2 \cdot b}{\pi \cdot a} \cdot \sin h\left(\frac{2 \cdot \pi \cdot a}{b}\right)\right] \cdot \boxed{K_2}$$

Segmente / Segments	$\boxed{K_1}$	$\boxed{K_2}$
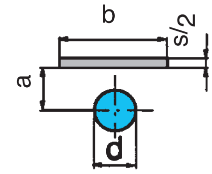	1	1
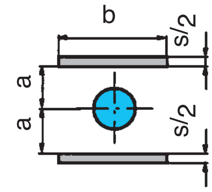	2	0.5
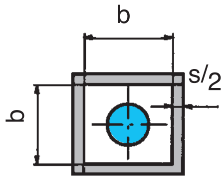	$4 + 2 \, \frac{s}{b}$	$\frac{0.077 + \ln\left(\frac{b}{d}\right)}{2 + \ln\left(\frac{b}{d}\right)}$ $a = \frac{b}{2}$
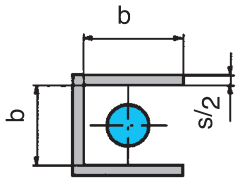	$3 + \frac{s}{2 \cdot b}$	$\frac{4}{3} \cdot \frac{0.077 + \ln\left(\frac{b}{d}\right)}{2 + \ln\left(\frac{b}{d}\right)}$ $a = \frac{b}{2}$
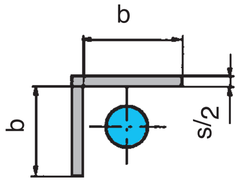	$2 + \frac{s}{2 \cdot b}$	$2 \cdot \frac{0.077 + \ln\left(\frac{b}{d}\right)}{2 + \ln\left(\frac{b}{d}\right)}$ $a = \frac{b}{2}$

Fig. 45: Heat conduction resistances and heat flows for square cooling segments [10]

2. Calculation of the heat conduction resistance from the surface of the heating/cooling channel to the heating/cooling medium

   Heat transfer resistance:

$$\text{WÜW} = \frac{1}{A_{TK} \cdot \alpha}$$

A_{TK}: surface of heating/cooling channel
α: coefficient of heat transfer

A correction factor is introduced for the coefficient of heat transfer that prevails in real-life heating/cooling elements.

$\alpha = \alpha^* \cdot K_f$

α^*: uncorrected coefficient of heat transfer
K_f: correction factor

$K_f = K_{fh} \cdot K_{fe} . K_{fg}$
K_{fe}; K_{fg}: correction factors, dependent upon the heating-/cooling segments

$$K_{f\eta} = \left(\frac{\eta\,(\bar{\vartheta})}{\eta\,(\vartheta_{TK})}\right)^{0.14}$$

$\eta(\bar{\vartheta})$ = dynamic toughness of the heating/cooling medium at the temperature which represents the average of the inflow and outflow temperature

$\eta(\vartheta_{TK})$ = dynamic toughness of the average local temperature of the heating/cooling channel wall

The design of the heating/cooling system can be approached in a highly flexible manner with the equations given for the heat flows per molding segment ($\dot{Q}_{FTS}$), for the heat conduction and heat transfer resistance and with the equations from the energy balance

$$\dot{Q}_{FTS} = \frac{1}{\text{WLW}} \left(\bar{\vartheta}_W - \vartheta_{TK}\right)$$

$$\dot{Q}_{FTS} = \frac{1}{1 + cp} \cdot \frac{1}{\text{WÜW}} \left(\vartheta_{TK} - \vartheta_{TM}\right)$$

$\bar{\vartheta}_W$ = mean cavity wall temperature
ϑ_{TK} = temperature of heating/cooling channel surface
ϑ_{TM} = temperature of heating/cooling medium

$$CP = \frac{\dot{Q}_U}{\dot{Q}_F}$$

The cavity wall temperature is always taken as the target parameter in the layout of a heating/cooling system. If the cooling medium and its temperature are specified (central cooling water facility or simply one cooling unit), the individual heating/cooling elements and segments should be designed in such a way that the heat conduction resistance is suitably aligned to the individual heat flows.

The segments inside the mold (sleeves) should be tackled first, since it is here that there are the least degrees of freedom. On outside segments, the heat conduction resistance can be more readily varied by changing the gap between the cooling channels.

The segmented heating/cooling system design makes it possible to allow for special features such as sudden changes in wall thickness and the corners of molded parts (Fig. 46).

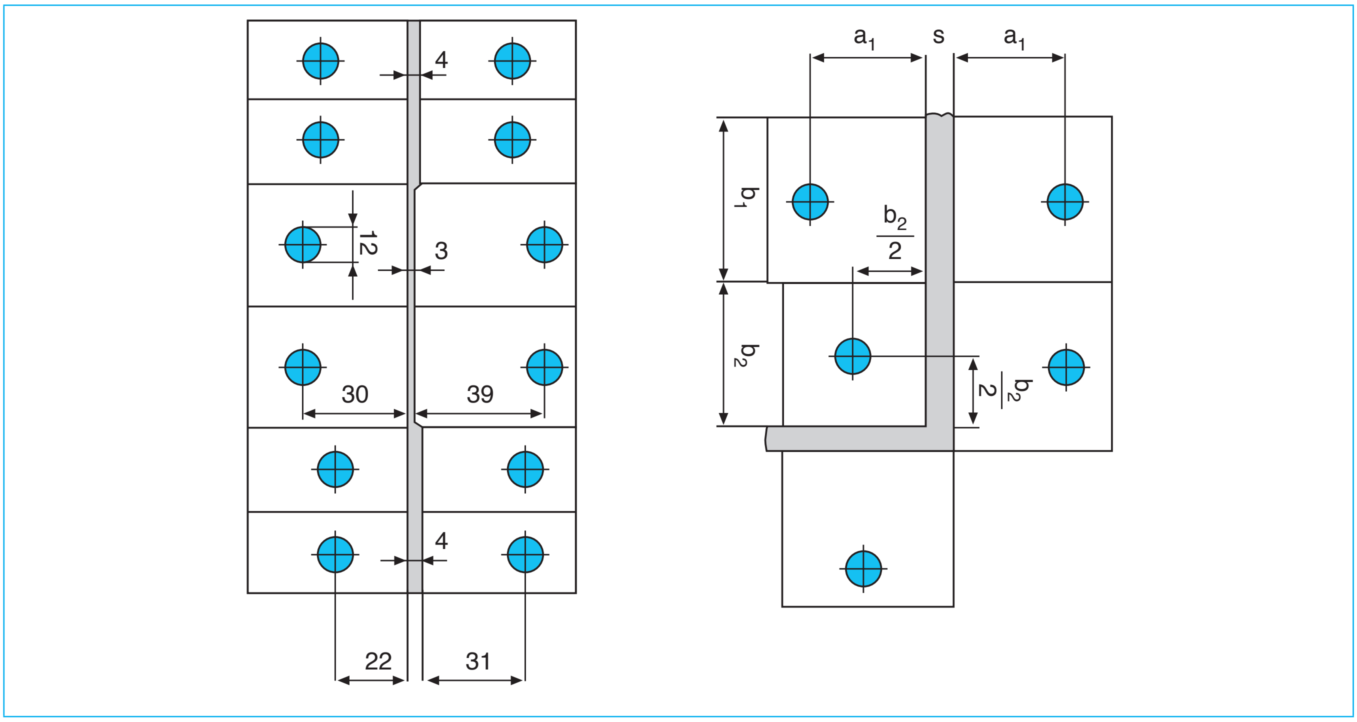

Fig. 46: Segmented heating/cooling system design: left: changes in wall thickness, right: molded part corners [10]

Temperierelement / Heating/cooling element	Beziehungen zur Wärmewiderstandsberechnung / Relation to the calculation of the heat transfer resistance
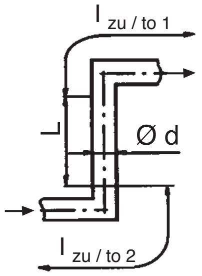	$d_h = d$ $A_{TK} = \pi \cdot d \cdot L$ $K_{fe} = \left(\frac{d_h}{L}\right)^{\frac{2}{3}} + 1$ $K_{fg} = 1$
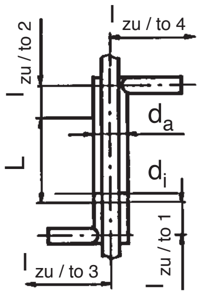	$d_h = d_a - d_i$ $A_{TK} = \pi \cdot d_a \cdot L$ $K_{fe} = \left(\frac{d_h}{L}\right)^{\frac{2}{3}} + 1$ $K_{fg} = \left(1 - 0.1\,\frac{d_i}{d_a}\right)$
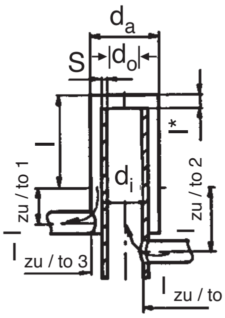	$d_h = d_a - d_i$ $A_{TK} = \pi \cdot d_a \cdot L$ $K_{fe} = \left(\frac{d_h}{L}\right)^{\frac{2}{3}}$ $K_{fg} = \left(1 - 0.1\,\frac{d_i}{d_a}\right)$
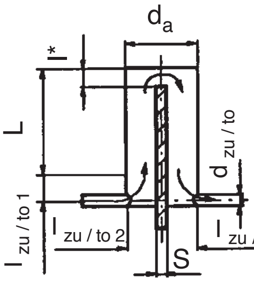	für / for s << d $d_h = \frac{\pi \cdot d_a}{2 + \pi} = 0.611 \cdot d_a$ $A_{TK} = (\pi \cdot d_a - 2 \cdot s) \cdot L$ $K_{fe} = 2 \cdot \left[\left(\frac{d_h}{L}\right)^{\frac{2}{3}} + 1\right]$ $K_{fg} = 1$

Fig. 47: Heating/cooling elements and heat transfer resistance [10]

12.3 Finite element analysis

To calculate the heating/cooling conditions by means of finite element analysis (boundary element analysis) it is necessary construct a three-dimensional computer model of the article, or cavity, and the heating/cooling channel geometry.

By introducing the outside cavity dimensions and making allowance for the ambient conditions, it is possible to calculate the flows of heat to the surroundings.

The advantages of finite element calculation over analytical calculations are as follows:

– solutions provided for complex geometries and for heat flows in more than one direction
– more precise simulation of the heating/cooling conditions
– readily comprehensible results (color plots)
– rapid run-through of variants (processing conditions heating/cooling channel configurations)
– a good link to computation modules for the filling and holding pressure phase and also to shrinkage and warpage programs

Fig. 48 shows the computer model of an electric drill housing (cavity) with the cooling channels on the nozzle and ejector side. The tool is depicted by the outline. The user can now specify the processing conditions:

– heating/cooling medium (e.g. water, oil, glycol)
– temperature of heating/cooling temperature (inflow)
– flow of heating/cooling medium

The program calculates the temperature conditions that prevail in the mold in the quasi-stationary state, including:

– cavity surface temperature, nozzle side (Fig. 49)
– cavity surface temperature, ejector side (Fig. 50)
– mean temperature of the molded part upon demolding (Fig. 51)

The programs also take in the temperature conditions in the cores and slides. In this way, allowance can be made for different mold materials (steel, copper-beryllium), and their influence on heat dissipation in the mold can be calculated.

Fig. 52 shows the calculated temperatures of a mold core that was not cooled (top left) and a mold core that was cooled with two baffle-plate cooling channels. At the top right, the core was made of steel while, at the bottom right, the core was made of a copper-beryllium alloy with a thermal conductivity of 120 W/(m · K).

In many cases, it is sufficient to conduct a thermal investigation of specific areas of the mold. In order to do this, it is possible to take a section through a specific point of the mold and use this as a computation model. As is shown in Fig. 53 by way of example, the heating/cooling in the corner of the molding can be optimized in this way.

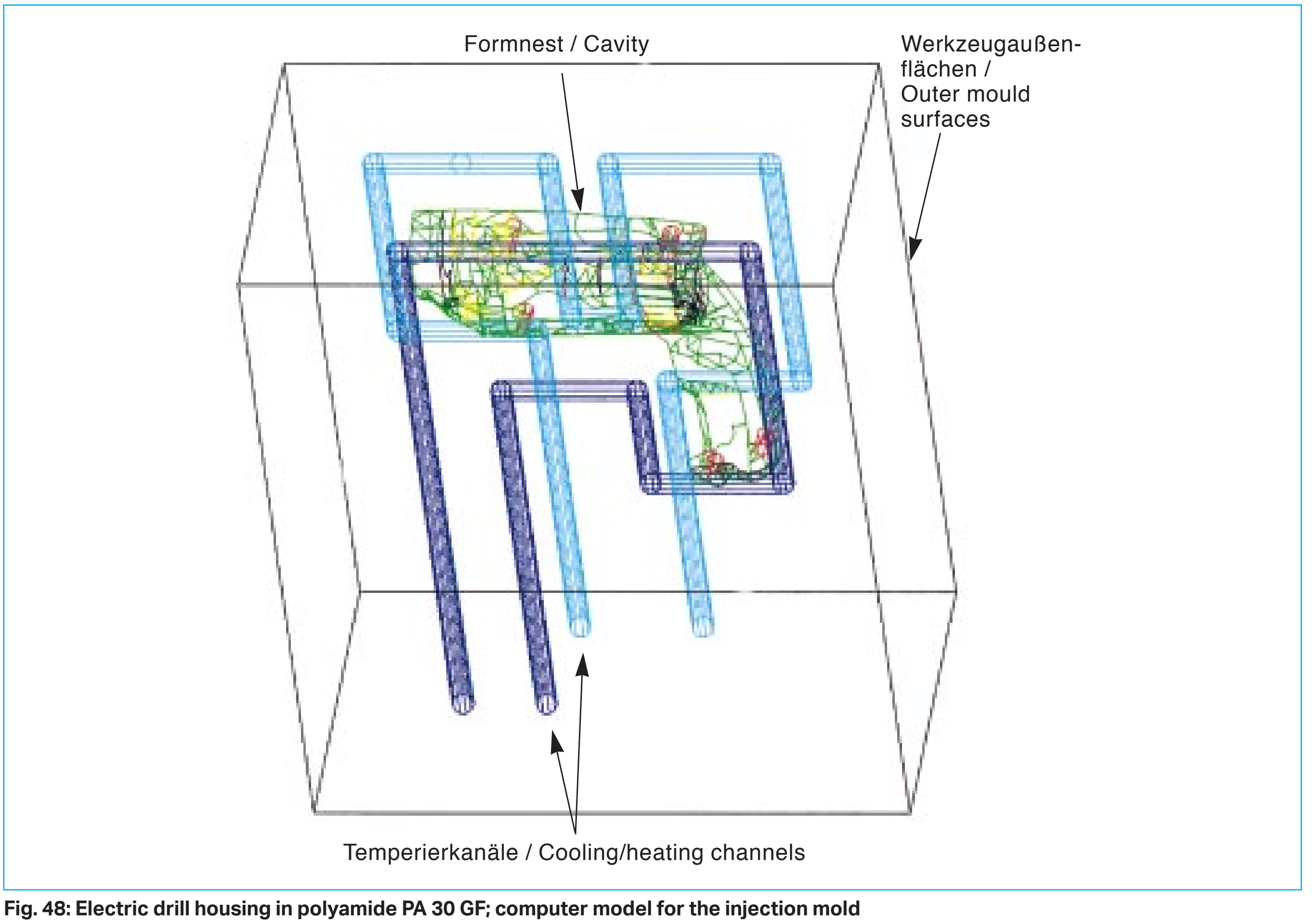

Fig. 48: Electric drill housing in polyamide PA 30 GF; computer model for the injection mold

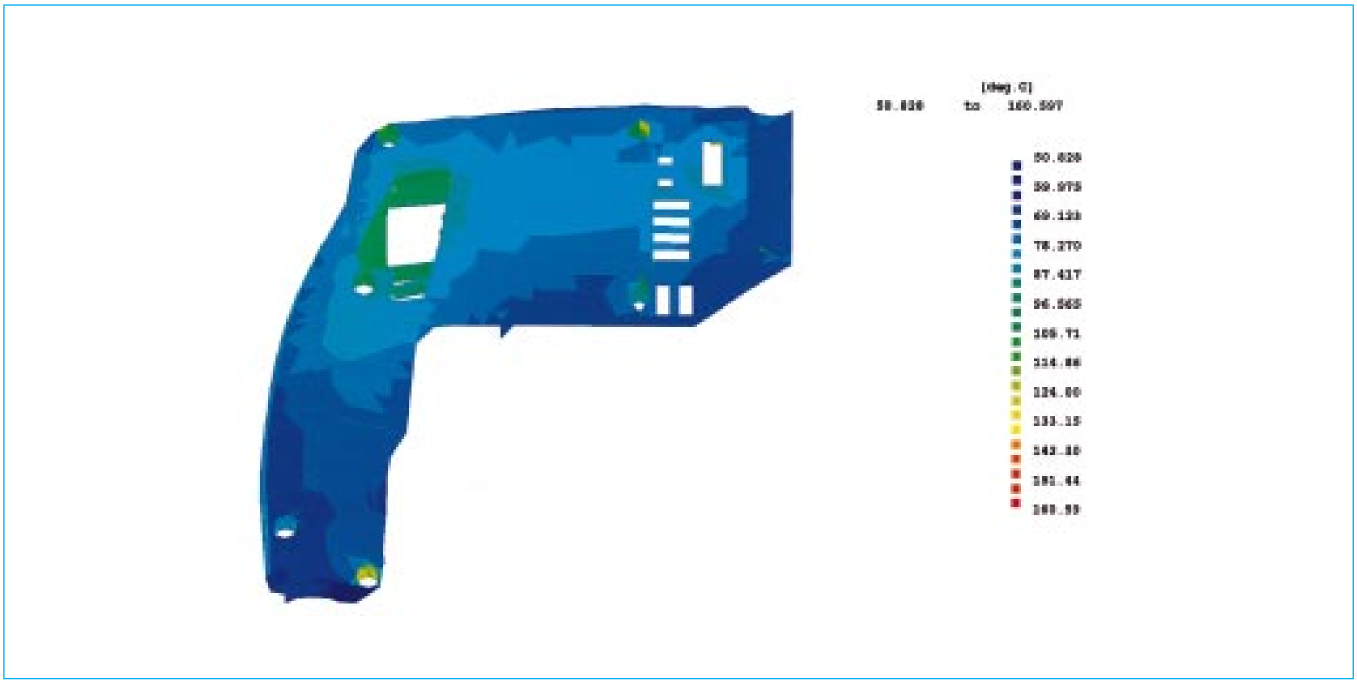

Fig. 49: Electric drill housing in polyamide PA 30 GF; computed surface temperatures on the nozzle side

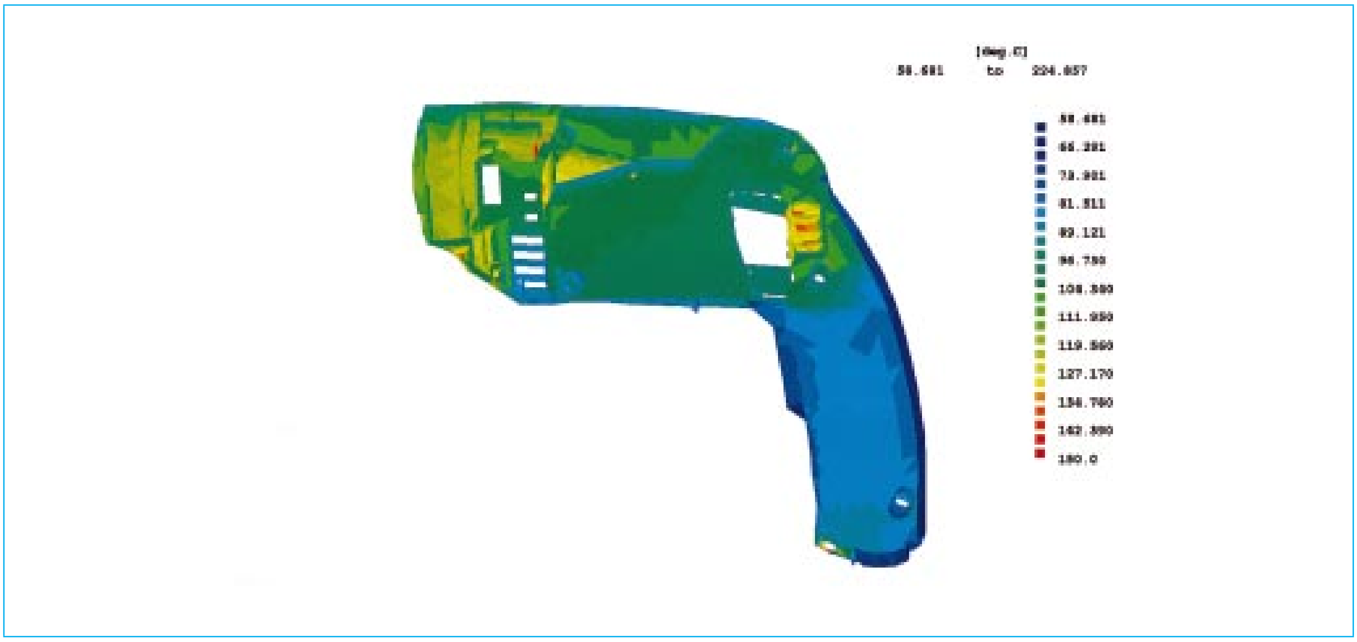

Fig. 50: Electric drill housing in polyamide PA 30 GF; computed surface temperatures on the ejector side

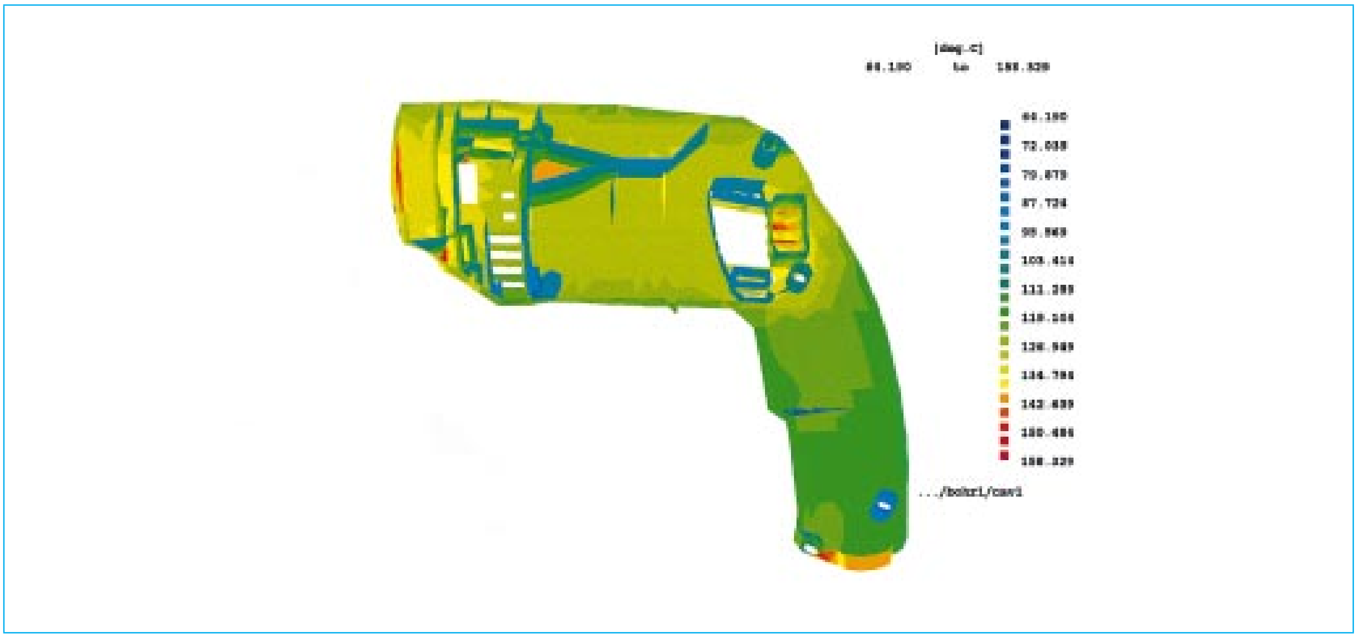

Fig. 51: Electric drill housing in polyamide PA 30 GF; computed mean temperatures in the plastic upon demolding

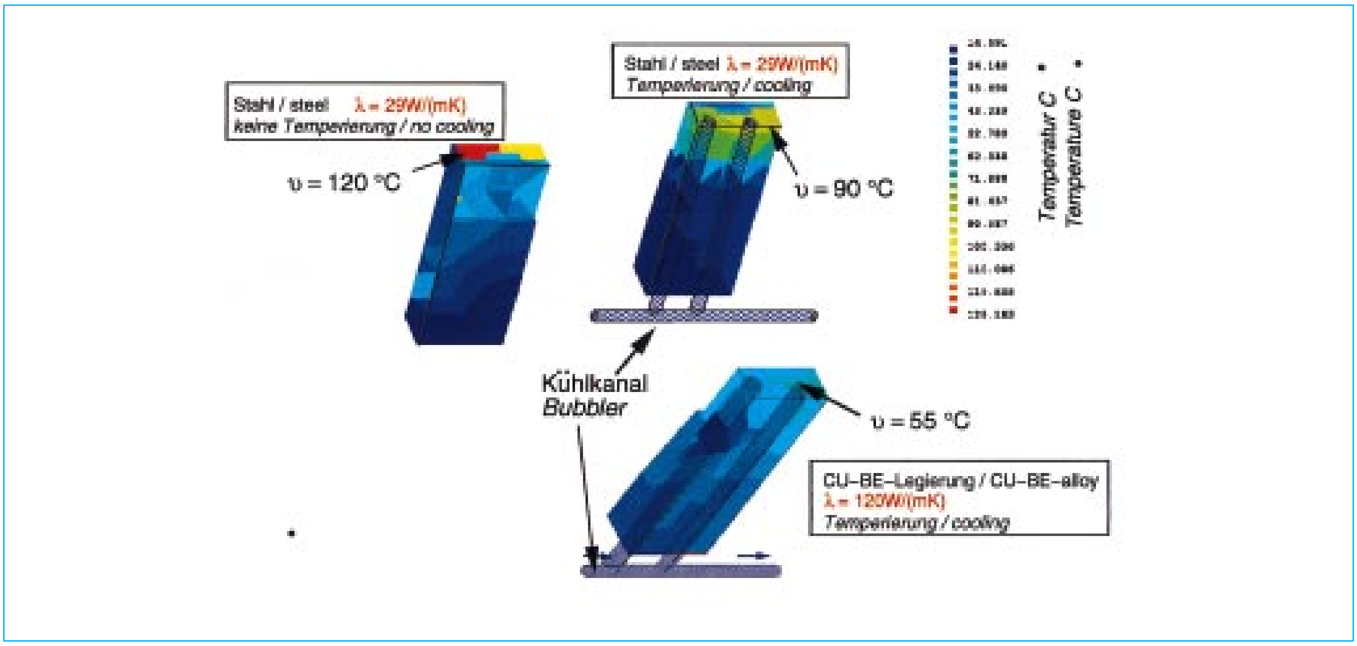

Fig. 52: Computed temperature distribution on a mold core (cooled and non-cooled, in steel and in a copper-beryllium alloy)

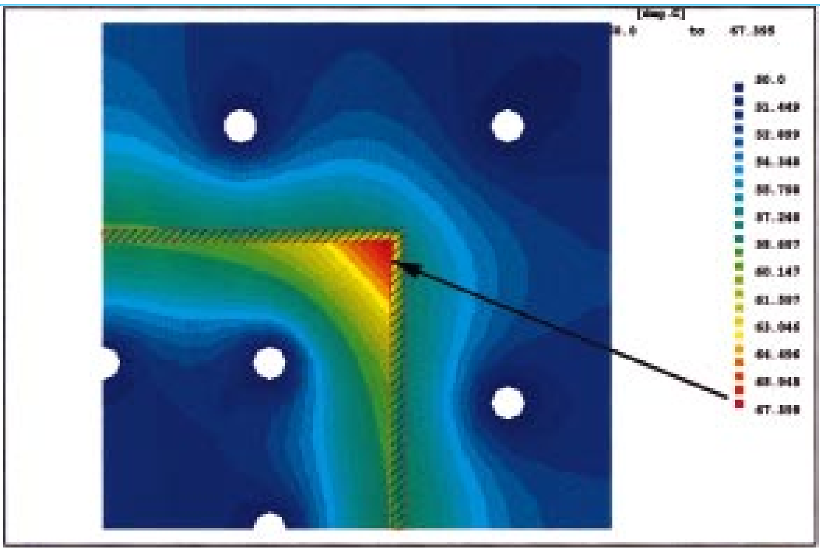

Istzustand /
Actual condition

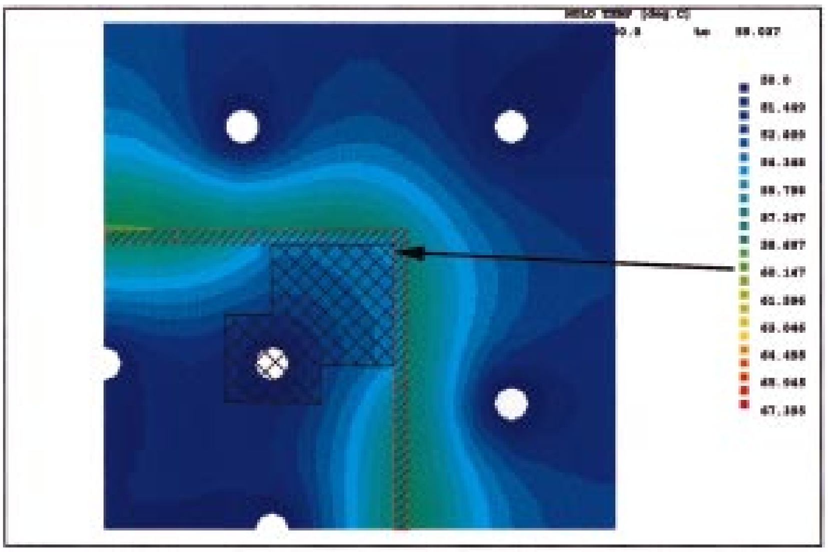

CU-BE-Einsatz /
CU-BE-insert

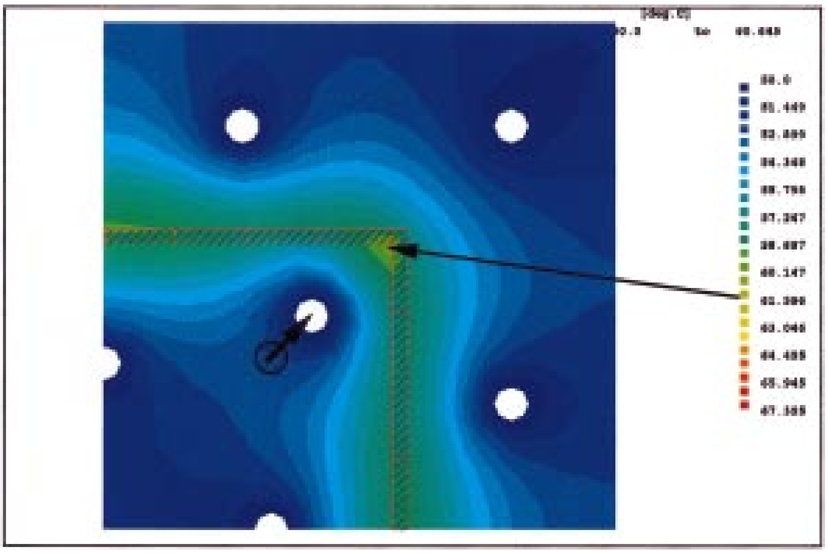

Temperierkanalverlegung /
Relocation of heating/cool-
ing channel

Fig. 53: Optimization of the heating/cooling system in a corner of the mold

13 Infrared photographs

Apart from performing a computer simulation of the thermal conditions prevailing in an injection mold, it is also possible to employ photographic techniques (infrared photographs) to rapidly detect imperfections in the heating/cooling.

Fig. 54 shows two infrared photographs, the left-hand one taken prior to optimization and the right-hand one taken after optimization of the heating/cooling conditions for the hood of a power brush made in ABS (Fig. 55).

Istzustand / actual condition
Zykluszeit / Cycle time 40 sec.

Optimierte Temperierung /
Optimised temperature control (System Contura®)
Zykluszeit / Cycle time 31 sec.

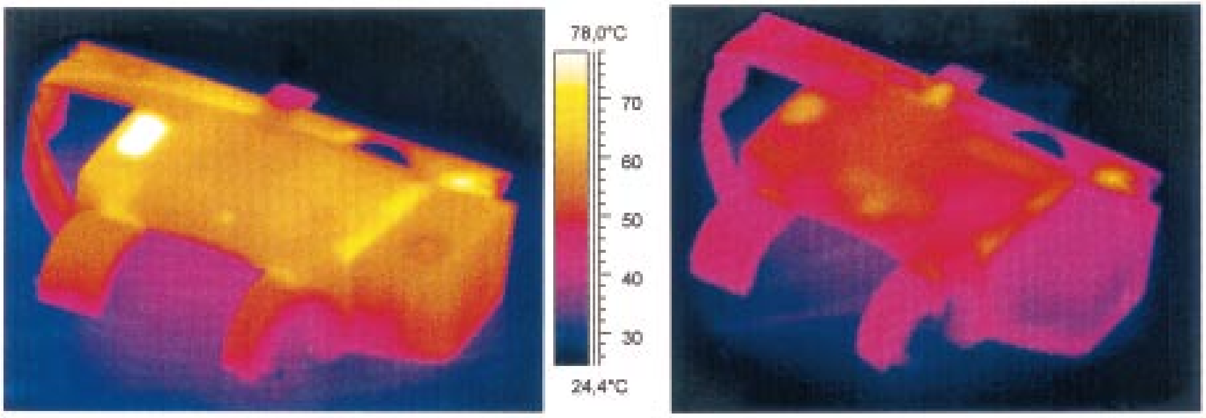

Fig. 54: Temperature distribution on the molded part surface photographed directly after demolding; source: Innova Engineering/ System CONTURA®

Fig. 55: Hood in ABS

In Fig. 54, the left-hand photograph shows temperatures ranging between 42 °C and 78 °C. With identical wall thicknesses in the molded part, this would suggest uneven heating/cooling in the mold. More uniform surface temperatures are obtained through optimization of mold cooling (Fig. 54, right-hand side). The critical temperature peaks become less pronounced. With this optimized heating/cooling, it proved possible to shorten the cycle time by approximately 9 s.

The different heat contents of the various areas of the molded part are made visible here by infrared photographs. Immediately after demolding, the temperature profiles prevailing over the wall of the molded part level out, and the heat from the inside layers reaches the surface of the molded part (Fig. 56 shows this in qualitative terms).

Apart from infrared photographs of the demolded injection molded parts, photographs of this type can also be taken of the cavity surface. The amount of preparation involved here, however, is much higher.

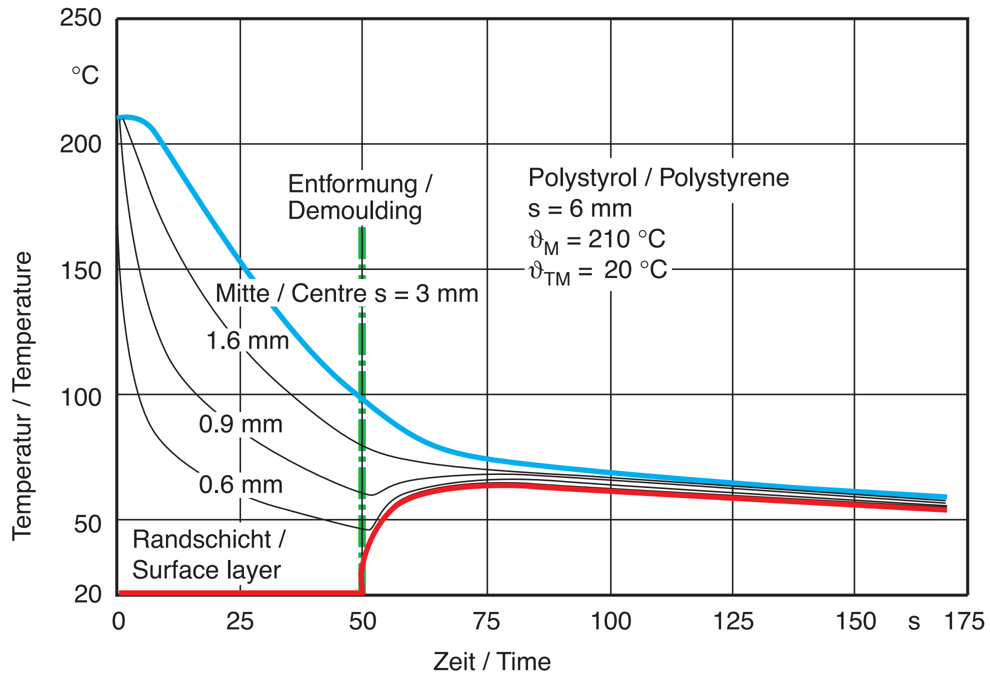

Fig. 56: Temperature profile in a plastic molded part before and after demolding

14 Conclusion

Injection molds that have been intelligently designed from the thermal angle help to bring down the cost of production while ensuring greater reliability. A large number of aids are currently available to design engineers, together with the results of theoretical and practical investigations which can be used in the thermal design of the mold.

In order to attain the specified aims of thermal mold design, i.e.

– precise maintenance of the target mean cavity temperature
– uniform distribution of the cavity temperature
– short cycle time with a high molding quality

the design engineer must be familiar with the temperature conditions that prevail in the mold and be able to influence these in the desired manner through the position of the heating/cooling channels.

Apart from determining the correct position of the heating/cooling channels, it is then equally important to establish the pressure losses in the heating/cooling channels and to select a heating/cooling unit with sufficient capacity. Only when a sufficient heating/cooling medium flow is available will the heat be eliminated from the mold (or be supplied to the mold in the case of heating).

The analytical equations and finite element programs can be used to check and improve on the heating/cooling of the mold. Specialist design engineers are called for here, who must be familiar with the theoretical correlations and have experience in the application of the calculations. The increased outlay on design, however, is very rapidly offset by the improvement in production.

15 Abbreviations

A = area and symbols used
A_A = mold platen area
A_F = molded part surface
A_{KK} = cooling channel surface
A_S = outer surface of mold
A_{TR} = mold parting plane
a = thermal conductivity
a_{eff} = effective thermal conductivity
B = distance between centerlines of cooling channels
Bi = Biot number (dimensionless)
b = heat permeability
b_M = heat permeability thermoplastic
b_W = heat permeability mold steel
c = specific heat capacity
C_S = radiation coefficient of black body
C_S = const. = 5,77 W/($m^2 \cdot K^4$)
c_{TM} = specific heat capacity of heating/cooling medium
C = distance between centerline of cooling channel and cavity wall
D_{HY} = hydraulic diameter
D_{KK} = diameter of cooling channels
h_1, h_2 = enthalpy at different temperatures
j = heating/cooling error
l_F = pro rata cavity height
l_{TK} = overall cooling channel length in mold or parts of mold
m = mass of molded part
$\dot{m}_{PU}$ = pump capacity (throughput) for heating/cooling system used
$\dot{m}_{TM}$ = mass flow of heating/cooling medium
$n_{B\sigma}$ = number of curves in heating/cooling circuit
n_{KN} = number of bends in heating/cooling circuit
n_{FT} = number of molded parts
N_P = requisite pump capacity
Nu = Nusselt number (dimensionless)
pBö = pressure loss in 90 ° curve
p_{tot} = overall pressure loss in the heating/cooling channels
p_{KK} = pressure loss in the cooling channel holes
p_{KN} = pressure loss in 90 ° bends
Pr = Prandtl number
$\dot{Q}_H$ = additional heat flow (hot runner manifold block)
$\dot{Q}_F$ = molded part heat flow
$\dot{Q}_K$ = heat flow due to convection
$\dot{Q}_{TM}$ = heat flow of heating/cooling medium
$\dot{Q}_{Str}$ = heat radiation
$\dot{Q}_U$ = exchange of heat with the surroundings
$\dot{Q}_L$ = heat flow due to conduction
$\dot{q}_K$ = heat flow density with convection
$\dot{q}_{Str}$ = heat flow density with radiation
Re = Reynolds number (dimensionless)
S = molded part wall thickness
s^2 = square of wall thickness
t = time
t_K = cooling time
t_{off} = mold open time
t_{cycle} = cycle time
T_M = mold temperature
T_U = absolute ambient temperature around mold ϑ_U + 273 °C
T_{WA} = absolute outside temperature of mold ϑ_{WA} + 273 °C
$\overline{T}_E$ = average demolding temperature
$\overline{T}_W$ = average mold surface temperature
U = circumference
v_{TM} = velocity of heating/cooling medium
α_L = coefficient of heat transfer for conduction [8 bis 15 W/$m^2 \cdot$ °C]
α_{TM} = coefficient of heat transfer for heating/cooling medium
β = coefficient of heat transfer for mold material
β_{isol} = coefficient of heat transfer for the insulating plate
ε = radiation coefficient
η_{TM} = dynamic toughness of heating/cooling medium
ρ = density
ϑ = temperature
$\Delta\vartheta_1$ = temperature differential due to heat conduction
$\Delta\vartheta_2$ = temperature differential due to heat transfer
ϑ_E = demolding temperature
$\hat{\vartheta}_E$ = maximum demolding temperature
ϑ_{KK} = temperature at cooling channel surface
ϑ_U = ambient temperature
ϑ_{IN} = inlet temperature of the heating/cooling medium
ϑ_{OUT} = outlet temperature of the heating/cooling medium
ϑ_M = melt temperature after completion of mold filling
$\Delta\vartheta_W$ = difference of mold surface temperature
$\Delta\vartheta_{Wij}$ = heating/cooling error
ϑ_W = mold surface temperature
$\overline{\vartheta}_W$ = mean mold wall temperature
ϑ_{WE} = mold outer surface
ϑ_{Wmax} = maximum mold surface temperature
ϑ_{Wmin} = minium mold surface temperature
ϑ_{TM} = temperature of heating/cooling medium
λ = thermal conductivity
λ_{isol} = thermal conductivity of insulating plate
λ_{TM} = thermal conductivity of heating/cooling medium

ν = kinematic toughness of heating/cooling medium
ζ = coefficient of friction for pipe flow
ζ_{Bo} = coefficient of friction for curves (≈ 0,4)
ζ_{KN} = coefficient of friction for bends (≈ 1,8)
ρ_{TM} = density of heating/cooling medium
Θ = degree of cooling
δ = distance between cooling channel and mold wall

16 References

[1] Verarbeitungsdaten für den Spritzgießer Informationsschrift, Covestro Deutschland AG, Leverkusen

[2] Wübken, G.: Einfluss der Verarbeitungsbedingungen auf die innere Struktur thermoplastischer Spritzgussteile unter besonderer Berücksichtigung der Abkühlverhältnisse.
Dissertation, RWTH Aachen, 1974

[3] Knappe, W.: Die Festigkeit thermoplastischer Kunststoffe in Abhängigkeit von den Verarbeitungsbedingungen.
Kunststoffe Bd. 51, 1961

[4] Stitz, S.: Analyse der Formteilbildung beim Spritzgießen von Plastomeren als Grundlage für die Prozesssteuerung.
Dissertation, RWTH Aachen, 1973

[5] Schauf, D.: Die strukturierte Formnestoberfläche und deren Abbildung durch Thermoplaste.
Anwendungstechnische Information ATI 584,
Bayer AG, Leverkusen

[6] Friel, P.: Werkzeugtemperierung und deren Einfluss auf die Eigenschaften der Fertigteile.
Beitrag: Das Spritzgießwerkzeug, VDI-Verlag GmbH

[7] Wübken, G.: Thermisches Verhalten und thermische Auslegung von Spritzgießwerkzeugen.
Herausgeber: Institut für Kunststoffverarbeitung an der RWTH Aachen, Juni 1976

[8] Thienel, P.: Rechnereinsatz (CAE) in der Spritzgießtechnik – thermische Auslegung von Spritzgießwerkzeugen.
Beitrag: Handbuch der Temperaturregelung mittels flüssiger Medien, Regloplas AG

[9] Schürmann, E.: Abschätzmethoden für die Auslegung von Spritzgießwerkzeugen.
Dissertation, RWTH Aachen, 1979

[10] Kretzschmar, O.: Rechnerunterstützte Auslegung von Spritzgießwerkzeugen mit segmentbezogenen Berechnungsverfahren.
Dissertation, RWTH Aachen, 1985

[11] Wübken, G. und Catic, I.: Nomogramm zur Bestimmung der Kühlzeit beim Spritzgießen.
Kunststoff-Berater, 1971, Nr. 9, Seite 779 – 783

[12] Wübken, G.: Berechnungsmöglichkeiten und Abschätzkriterien für die thermische Auslegung von Spritzgießwerkzeugen.
Beitrag: Das Spritzgießwerkzeug, VDI-Verlag GmbH

[13] Gastrow, H.: Der Spritzgießwerkzeugbau",
Carl Hanser Verlag

[14] Lichius und Schmidt.: Rechnerunterstütztes Konstruieren von Spritzgießwerkzeugen.
Vogel-Buchverlag, Würzburg

[15] Mink, G.: Grundlage der Spritzgießtechnik.
5. Auflage, Zechner & Hüthig Verlag GmbH,
Speyer am Rhein

Covestro Deutschland AG
Business Unit Polycarbonates
D-51365 Leverkusen, Germany

plastics@covestro.com
www.plastics.covestro.com